Neurobiology of Disease

Activation of PPARα Exhibits Therapeutic Efficacy in a Mouse Model of Juvenile Neuronal Ceroid Lipofuscinosis

Malabendu Jana,[1,2] **Debashis Dutta,**[1] **Jit Poddar,**[1] **and Kalipada Pahan**[1,2]

[1]Department of Neurological Sciences, Rush University Medical Center, Chicago, Illinois 60612 and [2]Division of Research and Development, Jesse Brown Veterans Affairs Medical Center, Chicago, Illinois 60612

Juvenile neuronal ceroid lipofuscinosis (JNCL) is a fatal inherited neurodegenerative disease of children that occurs because of defective function of the lysosomal membrane glycoprotein CLN3. JNCL features glial activation and accumulation of autofluorescent storage material containing subunit c of mitochondrial ATP synthase (SCMAS), ultimately resulting into neuronal loss. Until now, no effective therapy is available for JNCL. This study underlines the possible therapeutic importance of gemfibrozil, an activator of peroxisome proliferator-activated receptor α (PPARα) and a lipid-lowering drug approved by the Food and Drug Administration in an animal model of JNCL. Oral gemfibrozil treatment reduced microglial and astroglial activation, attenuated neuroinflammation, restored the level of transcription factor EB (TFEB; the master regulator of lysosomal biogenesis), and decreased the accumulation of storage material SCMAS in somatosensory barrel field (SBF) cortex of Cln3$^{\Delta ex7/8}$ (Cln3ΔJNCL) mice of both sexes. Accordingly, gemfibrozil treatment also improved locomotor activities of Cln3ΔJNCL mice. While investigating the mechanism, we found marked loss of PPARα in the SBF cortex of Cln3ΔJNCL mice, which increased after gemfibrozil treatment. Oral gemfibrozil also stimulated the recruitment of PPARα to the *Tfeb* gene promoter *in vivo* in the SBF cortex of Cln3ΔJNCL mice, indicating increased transcription of *Tfeb* in the CNS by gemfibrozil treatment via PPARα. Moreover, disease pathologies aggravated in Cln3ΔJNCL mice lacking PPARα (Cln3ΔJNCL$^{\Delta PPAR\alpha}$) and gemfibrozil remained unable to decrease SCMAS accumulation, reduce glial activation, and improve locomotor performance of Cln3ΔJNCL$^{\Delta PPAR\alpha}$ mice. These results suggest that activation of PPARα may be beneficial for JNCL and that gemfibrozil may be repurposed for the treatment of this incurable disease.

Key words: **gemfibrozil; glial activation; JNCL; lysosomal storage disorder; PPARalpha; storage materials**

Significance Statement

Despite intense investigations, no effective therapy is available for JNCL, an incurable inherited lysosomal storage disorder. Here, we delineate that oral administration of gemfibrozil, a lipid-lowering drug, decreases glial inflammation, normalizes and/or upregulates TFEB, and reduces accumulation of autofluorescent storage material in SBF cortex to improve locomotor activities in Cln3$^{\Delta ex7/8}$ (Cln3ΔJNCL) mice. Aggravation of disease pathology in Cln3ΔJNCL mice lacking PPARα (Cln3ΔJNCL$^{\Delta PPAR\alpha}$) and inability of gemfibrozil to decrease SCMAS accumulation, reduce glial activation, and improve locomotor performance of Cln3ΔJNCL$^{\Delta PPAR\alpha}$ mice delineates an important role of PPARα in this process. These studies highlight a new property of gemfibrozil and indicate its possible therapeutic use in JNCL patients.

Introduction

Juvenile neuronal ceroid lipofuscinosis (JNCL), or Batten disease, is a fatal autosomal recessive inherited childhood-onset neurodegenerative disorder caused by mutations in the *Cln3* gene (Greene et al., 1999; Mitchison et al., 1999; Cotman et al., 2002; Kim et al., 2017; Mirza et al., 2019; Petcherski et al., 2019; Rosenberg et al., 2019). With an estimated occurrence of 1 in 12,500 live births, JNCL is considered a rare neurologic disease. It usually begins between 4 and 10 years of age, with progressive visual deterioration, seizures, blindness, motor and cognitive decline, mental and intellectual deterioration, and epilepsy, ultimately ending with premature death during

Received Dec. 13, 2021; revised Dec. 29, 2022; accepted Jan. 9, 2023.

Author contributions: K.P. designed research; M.J., D.D., and J.P. performed research; M.J., D.D., and K.P. analyzed data; and K.P. wrote the paper.

This work was supported by National Institutes of Health–Center for Information Technology Grants AG050431 and AT010980, U.S. Department of Veterans Affairs Grant 1IK6 BX004982 (K.P.), and Polaryx Therapeutics (KP). We thank Dr. Bryan Killinger and Dr. Liudmila Romanova of the Department of Neurological Sciences, Rush University Medical Center, for help with confocal microscopy.

The authors declare no competing financial interests.

Correspondence should be addressed to Kalipada Pahan at Kalipada_Pahan@rush.edu.

https://doi.org/10.1523/JNEUROSCI.2447-21.2023

Table 1. Antibodies, sources, applications, and dilutions used

Antibody	Manufacturer	Catalog no.	Host	Application	Dilution
GFAP	Dako	20334	Rabbit	IF, WB	IF, 1:1000 WB, 1:2000
PPARα	Santa Cruz Biotechnology	sc-398394	Mouse	WB, IF, and ChIP	WB, 1:500 IF, 1:100 ChIP, 2 μg/10^6 cells
RNA-Pol II	Santa Cruz Biotechnology	sc-56767	Mouse	ChIP	2 μg/10^6 cells
CBP	Santa Cruz Biotechnology	sc-365387	Mouse	ChIP	2 μg/10^6 cells
IgG	Santa Cruz Biotechnology	sc-2025	Mouse	ChIP	2 μg/10^6 cells
Inducible nitric oxide synthase	BD Bioscience	610329	Mouse	WB and IF	WB, 1:500 IF, 1:500
IL-1β	Santa Cruz Biotechnology	sc-7884	Rabbit	WB	1:500
TNFα	Santa Cruz Biotechnology	sc-133192	Mouse	WB	WB, 1:500
TFEB	Abcam	ab2636	Goat	WB and IF	WB, 1:500 IF, 1:500
Subunit C of ATP synthase	Abcam	ab181243	Rabbit	IF	1:500
NeuN	Invitrogen	702022	Rabbit	IF	1:1000
Iba1	Abcam	ab107159	Goat	WB and IF	1:500
β-Actin	Abcam	ab8226	Mouse	WB	1:10000

WB, Western blot; IF, immunofluorescence; GFAP, glial fibrillary acidic protein; Iba-1, ionized calcium-binding adaptor molecule 1; IL-1β, interleukin 1β; TNFα, tumor necrosis factor α.

the second and third decade of life (Pohl et al., 2007; Kim et al., 2017; Shematorova and Shpakovski, 2020). The pathologic hallmark of JNCL is the accumulation of autofluorescent storage material containing subunit c of the mitochondrial F_0 ATP synthase complex, lipoproteins, and glycoproteins (Cao et al., 2011; Brenneman et al., 2017). Remarkably, depositions of F_0 ATP synthase complex are not only found in CNS neurons but are also abundant in non-neuronal cells outside the CNS (Katz et al., 1997). In addition, similar to that seen in other neurodegenerative disorders (Pahan et al., 1998; Roy et al., 2006; Saha and Pahan, 2006; Jana et al., 2008), glial activation is also a prominent feature of JNCL. Brain autopsies display that neuron loss is greatest where astroglial and microglial activation is most pronounced (Pontikis et al., 2005; Cooper et al., 2015; Parviainen et al., 2017; Lange et al., 2018). However, despite intense investigations, no effective therapy is available for JNCL.

Gemfibrozil is a lipid-lowering drug approved by the Federal Drug Administration (FDA) for its ability to reduce the level of triglycerides and to decrease the risk of hyperlipidemia. However, a number of recent studies from us and others have demonstrated that in addition to lipid lowering, gemfibrozil is capable of modulating multiple cellular processes. Gemfibrozil exhibits anti-inflammatory outcome by suppressing the expression of proinflammatory molecules (Pahan et al., 2002; Jana et al., 2007; Roy and Pahan, 2009; Jana and Pahan, 2012) and upregulating the expression of different anti-inflammatory molecules (Corbett et al., 2012; Ghosh et al., 2012) in astrocytes and microglia. Gemfibrozil displays immunomodulatory effect to switch T-helper 1 cells toward T-helper 2 (Dasgupta et al., 2007) and modify T cell-to-microglia contact (Roy et al., 2007) by altering the expression of surface molecules. Gemfibrozil can also stimulate the expression of myelin-specific genes (Jana et al., 2012) and attenuate the disease process of experimental autoimmune encephalomyelitis, an animal model of multiple sclerosis (Lovett-Racke et al., 2004; Dasgupta et al., 2007). It has been also shown that gemfibrozil treatment readily increases lysosomal biogenesis and autophagy (Ghosh et al., 2015) and thereby reducing plaque load in an animal model of Alzheimer's disease (Chandra and Pahan, 2019). Recently, we have demonstrated the neurotrophic property of gemfibrozil in which this drug protects dopaminergic neurons in a mouse model of Parkinson's disease via PPARα-dependent astrocytic GDNF pathway (Gottschalk et al., 2021).

The present investigation was conducted to examine whether gemfibrozil could halt and/or slow down the disease process of JNCL in $Cln3^{\Delta ex7/8}$ (Cln3ΔJNCL) mice. Here, we provide evidence that orally administered gemfibrozil markedly attenuated the glial activation, increased the level of TFEB to reduce the accumulation of subunit c of mitochondrial ATP synthase (SCMAS), and improved locomotor activities in $Cln3\Delta JNCL^{\Delta PPAR\alpha}$ mice via PPARα. These results suggest that gemfibrozil may have therapeutic importance in JNCL.

Materials and Methods

Reagents

Different molecular-biology-grade chemicals were obtained from Sigma-Aldrich. Gemfibrozil and methyl cellulose were purchased from Spectrum Chemicals. Primary antibodies, their sources, and the concentrations used are listed in Table 1. Alexa Fluor antibodies used in immunostaining were purchased from Jackson ImmunoResearch Laboratories. Infrared (IR)-dye-labeled reagents used for immunoblotting were received from Li-Cor Biosciences.

Animals and gemfibrozil treatment

Homozygous CLN3 ($Cln3^{\Delta ex7/8}$; The Jackson Laboratory) mice were used as a model of JNCL. These mice are referred to as Cln3ΔJNCL throughout the rest of the article. Cln3ΔJNCL mice were screened by genotyping that was performed by PCR on DNA obtained from tail biopsy samples using the following primers: common, 5′-CACTTGGGAGATTGTGAATTTG-3′; mutant reverse, 5′-GGTGCTCCCAGCCTCTAGGT-3′; and wild-type (WT) reverse, 5′-GAGATAGGGTTTTGCTGTGC-3′.

WT mice from the same background were used as controls. Cln3ΔJNCL mice were crossed with PPARα null mice to create $Cln3\Delta JNCL^{\Delta PPAR\alpha}$ bigenic mice. Animals were maintained and experiments were conducted in accordance with National Institutes of Health (NIH) *Guide for the Care and Use of Laboratory Animals* and were approved by the Rush University Medical Center Institutional Animal Care and Use Committee. Three-month-old Cln3ΔJNCL and $Cln3\Delta JNCL^{\Delta PPAR\alpha}$ mice of both sexes at equal ratio were treated with different dose of gemfibrozil (4 and 8 mg/kg body weight/d) solubilized in 100 μl 0.1% methyl cellulose (MC) via gavage for 3 months, followed by monitoring locomotor activity and biochemical assays. Another group of Cln3ΔJNCL mice also received only MC as vehicle.

Immunohistochemistry

For immunohistochemistry, mice were anesthetized and intracardially perfused with 1× PBS followed by 4% paraformaldehyde (PFA) in 0.1 M phosphate buffer, pH 7.4. The brains were postfixed in PFA overnight at 4°C and were then transferred to phosphate buffer containing 30% sucrose at 4°C. Somatosensory barrel cortex sections were cut and saved in serial order at −20°C until immunostained. For this, the hemi brains incubated in 30% sucrose were washed thoroughly in PBS and cryosectioned using a sliding microtome (American Optical 860). Before staining, 40 μM free-floating somatosensory barrel field (SBF) cortex sections were washed thoroughly in PBS. The sections were blocked using 2% BSA in PBSTT (PBS plus Triton X-100 plus Tween 20) for 1 h. Next, the sections were incubated with primary antibody in 1% PBSTT at 4°C overnight. The following day, sections were washed in PBSTT and incubated with Alexa Fluor 488 or 647 conjugated secondary antibody (Jackson ImmunoResearch Laboratories) for 3 h at room temperature. Following washes in PBSTT, the sections were mounted on glass slides (Patel et al., 2019; Raha et al., 2020). The samples were visualized under an Olympus BX41 fluorescence microscope equipped with a Hamamatsu ORCA-03G camera.

In some cases (e.g., TFEB and NeuN double labeling), images were acquired on a Nikon A1 confocal microscope with different objectives and resonant or galvano scanners. Imaging of larger fields was performed using a high-speed resonant scanner and long working distance 20× lens that allowed reasonable acquisition times. Imaging of the regions of interest with higher magnification was done using a galvano scanner with a 20× objective. Elements (Nikon) or Imaris software was used for processing and analyzing images. Imaging algorithms were tile scans with *z*-stack acquisition where *z*-section thickness varied from 20 to 1800 μm depending on the experiment. Whenever needed, maximum intensity or 3D projections were generated.

For DAB staining, somatosensory motor cortex sections were stained for GFAP and Iba1 using the Vectastain DAB protocol, mounted and observed under an Olympus brightfield microscope. Optical density measures were produced using ImageJ software (Raha et al., 2020; Paidi et al., 2021a) as described before (Varghese et al., 2014). Counting analysis was performed using Olympus MicroSuite V software for imaging applications with the help of a touch counting module (Corbett et al., 2015).

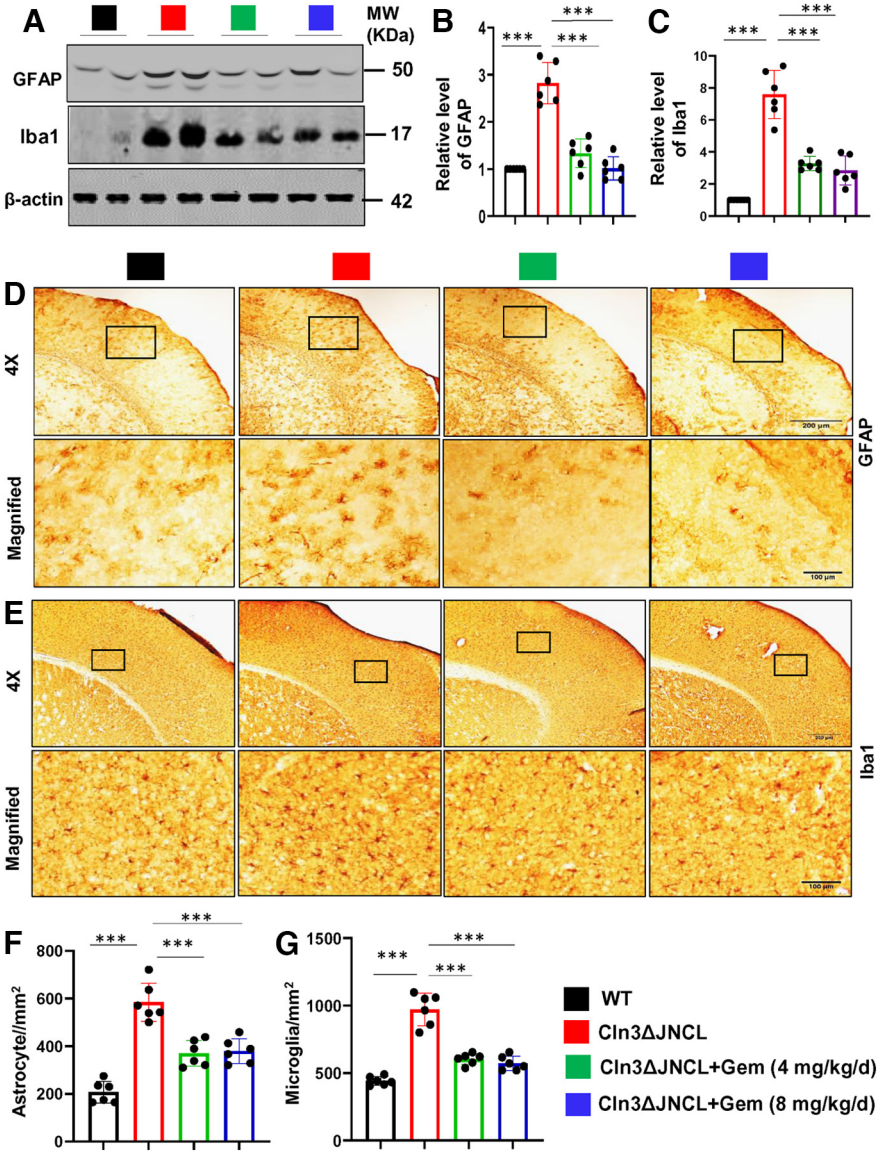

Figure 1. Effect of gemfibrozil on glial activation in the SBF cortex of $Cln3^{\Delta Ex7/8}$ (Cln3ΔJNCL) mice. ***A***, Three-month-old Cln3ΔJNCL mice ($n = 6$ per group) of both sexes at equal ratio were treated with different doses of gemfibrozil (4 and 8 mg/kg body weight) daily via gavage for 3 months followed by monitoring the protein level of different proinflammatory molecules by Western blot. ***B–E***, Bands were scanned and values (cytokine/actin) presented as relative to WT-control (***B***, GFAP; ***C***, Iba1). DAB staining of SBF cortical sections for GFAP (***D***) and Iba1 (***E***). ***F***, ***G***, GFAP-positive (***F***) and Iba-1-positive (***G***) cells were counted in one section (two images per section) of each of six different mice ($n = 6$) per group; $^{**}p < 0.01$; $^{***}p < 0.001$.

Immunoblotting

Western blotting was conducted as described elsewhere (Jana et al., 2012; Rangasamy et al., 2018; Chandra and Pahan, 2019). After 12 weeks of treatment, mice were perfused with PBS, and from a half part of the mice brain we collected somatosensory motor neuron region, homogenized in RIPA buffer. The supernatant was collected and analyzed for protein concentration via the Bradford method (Bio-Rad). SDS sample buffer was added to protein samples and boiled for 5 min. Denatured samples were electrophoresed on 10 or 12% Bis-Tris SDS polyacrylamide gels in a continuous buffer system, transferred onto a nitrocellulose membrane (Bio-Rad) using the Thermo-Pierce Fast Semi-Dry Blotter. The membrane was then washed for 15 min in TBS plus Tween 20 (TBST) and blocked for 1 h in TBST containing BSA. Next, membranes were incubated at 4°C under shaking conditions with primary antibodies followed by washing of membranes in TBST for 1 h. Membranes were then incubated in secondary antibodies for 1 h at room temperature, washed for 1 more hour, and visualized under the Odyssey Infrared Imaging System (Li-COR Biosciences). Blots were converted to binary, analyzed using ImageJ (NIH), and normalized to the β-actin loading control.

In situ *chromatin immunoprecipitation assay*

In situ chromatin immunoprecipitation (ChIP) was performed as described (Dutta et al., 2021; Paidi et al., 2021b). Briefly, animals were perfused with PBS and then PBS containing 4% paraformaldehyde, followed by isolation of somatosensory barrel field (SBF) cortex for the isolation of DNA using the phenol-chloroform-isopropyl alcohol method of DNA isolation. ChIP was performed on the cell lysate by overnight incubation at 4°C with 2 μg of anti-PPARα, anti-CREB-binding protein

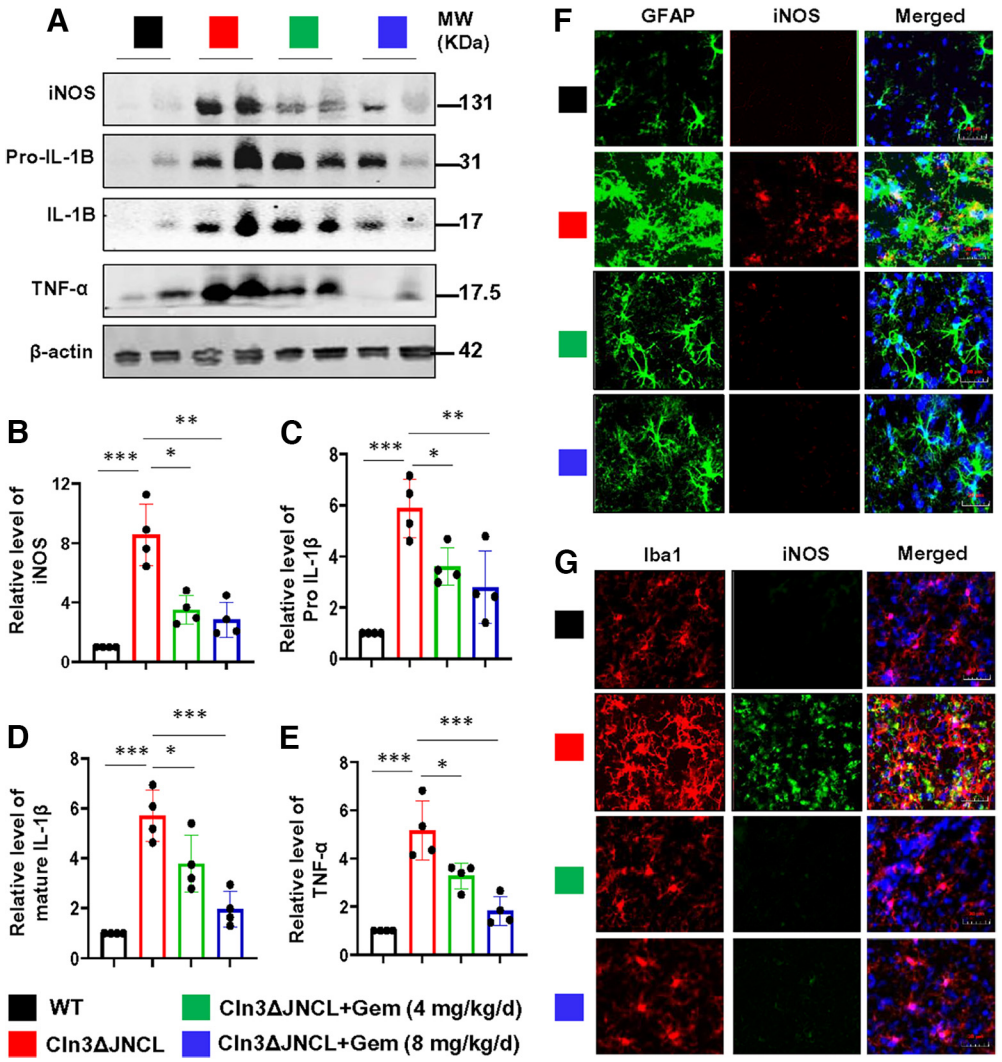

Figure 2. Effect of gemfibrozil on the level of different proinflammatory molecules in the SBF cortex of Cln3ΔJNCL mice. ***A***, Three-month-old Cln3ΔJNCL mice ($n = 6$ per group) of both sexes at equal ratio were treated with different doses of gemfibrozil (4 and 8 mg/kg body weight) daily via gavage for 3 months followed by monitoring the protein level of different proinflammatory molecules by Western blot. ***B–E***, Bands were scanned and values (cytokine/actin) presented as relative to WT-control (***B***, iNOS; ***C***, Pro-IL-1β; ***D***, IL-1β; ***E***, TNFα). ***F***, ***G***, Immunostaining of SBF cortical sections for GFAP (***F***) and Iba1 (***G***). Results represent analysis of one section of each of six different mice per group. Results are mean ± SEM of six mice per group; *$p < 0.05$; **$p < 0.01$; ***$p < 0.001$.

(CBP), or anti-RNA polymerase II antibodies followed by incubation with protein G agarose (Santa Cruz Biotechnology) for 2 h. The beads were then washed with cold IP buffer, and a total of 100 µl of 10% Chelex (10 × g/100 ml H_2O) was added to the washed protein G beads and vortexed. The Chelex/protein G bead suspension was boiled for 10 min and then allowed to return to room temperature. Proteinase K (100 µg/ml) was then added, and the beads were incubated for 30 min at 55°C while being shaken, followed by another round of boiling for 10 min. The suspension was centrifuged, and the supernatant was collected. This elute was used for conducting semiquantitative and real-time PCR. The fragment containing peroxisome proliferator response element (PPRE) of the mouse *Tfeb* promoter was amplified using the following primers: sense, 5′-GAA CAT TCC AGG TGG AGG CA-3′, antisense, 5’-CCC CCA ACA CAT GCT TCT CT-3′. For real-time PCR, data were normalized with the input, and the fold change with respect to the untreated control was calculated.

Behavioral Analyses

Open field test. The open field test was performed as described elsewhere (Patel et al., 2018; Raha et al., 2020; Paidi et al., 2021a). Briefly, each mouse was allowed to freely explore an open field arena for 5 min. The testing apparatus was a classic open field (i.e., a wooden floor square arena, 40 × 40 cm, with walls 30 cm high). A video camera (Basler GenICam acA1300-60) connected to a Noldus computer system was placed above the box. Each mouse was placed individually on the center of the arena, and the locomotor activity and other parameters like velocity, total distance traveled, and center time frequency was monitored for 5 min using a live video tracking system (Noldus). The central area was arbitrarily defined as a square of 20 × 20 cm (half the total area).

Rotarod test. The rotarod uses a motor-driven, rotating rod to measure limb motor coordination and balance of mice. It was measured on a rotarod apparatus (series ENV-576 M, Med Associates), using the protocol described previously (Chandra and Pahan, 2019; Patel et al., 2019; Raha et al., 2020). Briefly, mice were transported (within their home cage) to acclimate to the testing room for 1 h before trial. Before acquisition, the parameters of the rotarod system, equipped with automatic fall detector such as start speed and acceleration, were carefully checked before acquisition. Each mouse was placed on the confined section of the rod and the trial was initiated with a smooth increase in speed from 4 to 40 rpm for 5 min. If the mouse did not fall from the rod, it was removed from the rod after 5 min.

Pole test. To test motor coordination and spatial awareness, a vertical test was performed as described before (Chandra et al., 2016; Raha et al.,

2020). A vertical wooden pole with a rough surface (50 cm in height and 1 cm in diameter) was placed in the home cage. Mice were acclimatized to the pole over three trials of 120 s each. Each trial was separated by 60 s, and during behavioral testing, each mouse was tested three times.

Detection of storage materials

Detection of storage materials was performed by monitoring SCMAS by immunofluorescence as described before (Ghosh et al., 2017; Table 1 for details on antibody dilutions). DAPI was used to monitor nucleus. SCMAS associated fluorescence intensity was quantified by using Olympus MicroSuite V Software. Briefly, captured images were opened in the infinity image viewer and the contour was drawn around the granules to obtain the fluorescence intensity.

Densitometric analysis

Protein blots were analyzed using ImageJ software (NIH), and bands were normalized to their respective β-actin loading controls. Data are representative of the average fold change with respect to control for three independent experiments.

Statistical analysis

Statistical analyses were performed using GraphPad Prism 8.0 software (GraphPad). Mouse behavioral parameters were examined by an independent one-way ANOVA using IBM SPSS Statistics software. Homogeneity of variance between test groups was examined using Levene's test. *Post hoc* analyses were conducted using Tukey's test. Other data were expressed as means ± SD of three independent experiments. Statistical differences between means were calculated by Student's *t* test (two tailed). A *p* value of <0.05 ($p < 0.05$) was considered statistically significant.

Results

Oral administration of gemfibrozil attenuates glial activation in SBF cortex of Cln3ΔJNCL mice

Several studies have demonstrated neuroinflammation in the CNS of different CLN mouse models (Tyynelä et al., 2004; Xiong and Kielian, 2013; Groh et al., 2017; Kim et al., 2017; Rosenberg et al., 2019; Shematorova and Shpakovski, 2020; Specchio et al., 2021). Because gemfibrozil inhibits glial activation and associated inflammation (Pahan et al., 2002; Jana et al., 2007), we investigated whether gemfibrozil treatment was capable of suppressing astroglial activation in an animal model of JNCL. Although multiple mouse models of JNCL have been generated affecting the orthologous murine *Cln3* gene to mimic the human mutation, $Cln3^{\Delta ex7/8}$ knock-in mice leading to 1.02 kb genomic deletion in the *Cln3* eliminates exons 7 and 8 surrounding intronic DNA corresponds to the most common deletion found in JNCL patients (Mitchison et al., 1999; Cotman et al., 2002; Cao et al., 2006; Kyttälä et al., 2006; Pohl et al., 2007). Therefore, here, we used $Cln3^{\Delta ex7/8}$ knock-in (Cln3ΔJNCL) mice to study the efficacy of gemfibrozil. We focused mainly on SBF cortex because widespread glial activation is seen in SBF cortex of Cln3ΔJNCL mice (Bosch et al., 2016). As expected, an increased protein level of astroglial marker GFAP was seen in SBF cortex of 6-month-old Cln3ΔJNCL mice compared with age-matched WT mice (Fig. 1*A*,*B*). However, oral administration of different doses (4 and 8 mg/kg body weight/d) of gemfibrozil strikingly reduced the level of GFAP protein (Fig. 1*A*,*B*). Immunohistochemical

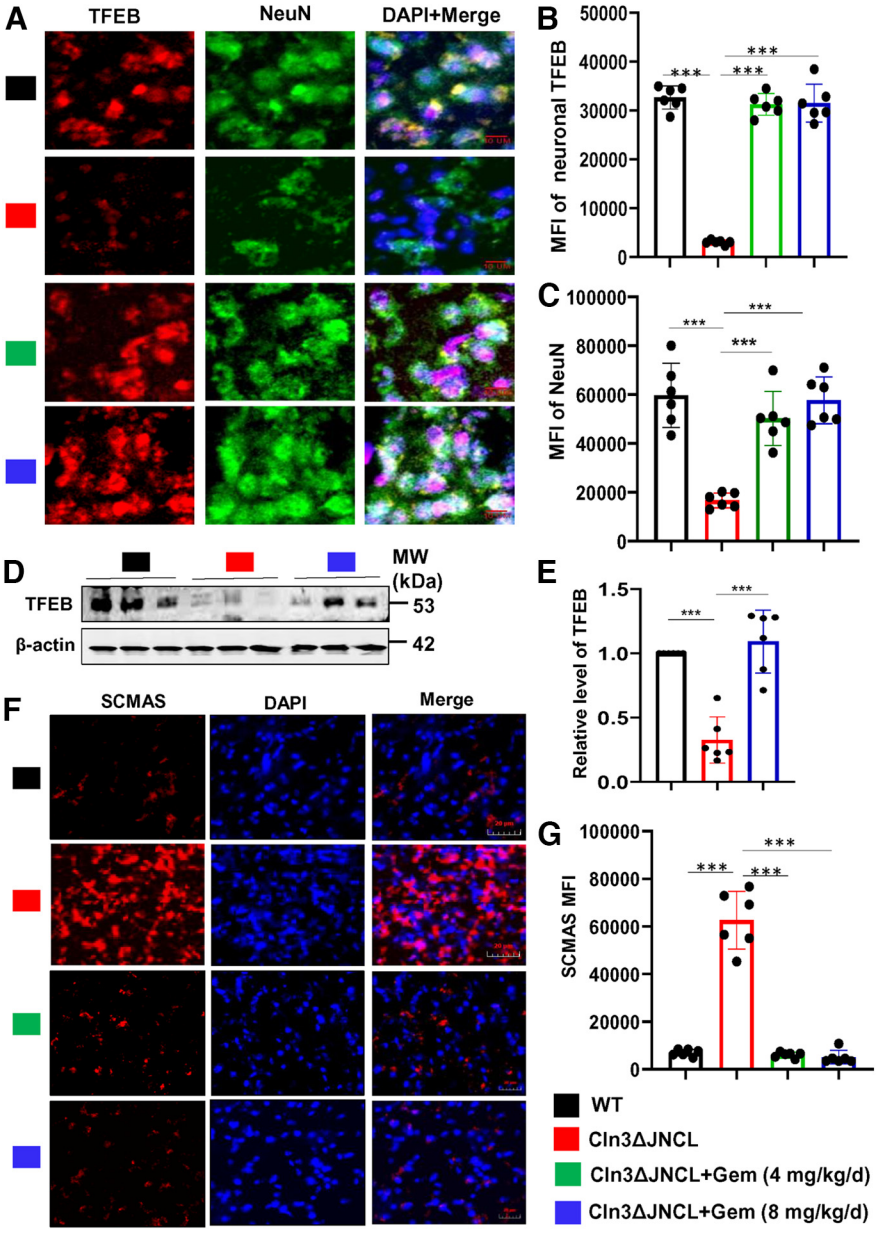

Figure 3. Effect of gemfibrozil on the level of TFEB and storage materials in the SBF cortex of Cln3ΔJNCL mice. ***A***, Three-month-old Cln3ΔJNCL mice ($n = 6$ per group) of both sexes at equal ratio were treated with different doses of gemfibrozil (4 and 8 mg/kg body weight) daily via gavage for 3 months followed by double labeling of SBF cortical sections with antibodies against TFEB and NeuN. Images were obtained with 20× magnification in Nikon A1 confocal microscope. ***B***, ***C***, MFI of TFEB (***B***) and NeuN (***C***) was quantified in two different sections (2 images per section) of each of six different mice ($n = 6$) per group using NIH ImageJ software. ***D***, SBF cortical homogenates were immunoblotted for TFEB. Actin was run as a loading control. ***E***, Bands were scanned and values (TFEB/actin) presented as relative to WT-control. Results are mean ± SEM of six mice per group. ***F***, Storage pigments were observed in SBF cortical sections by immunofluorescence analysis of SCMAS. DAPI was used to visualize nucleus. ***G***, MFI of SCMAS was quantified in one section (2 images per section) of each of six different mice ($n = 6$) per group using NIH ImageJ software; $^{***}p < 0.001$.

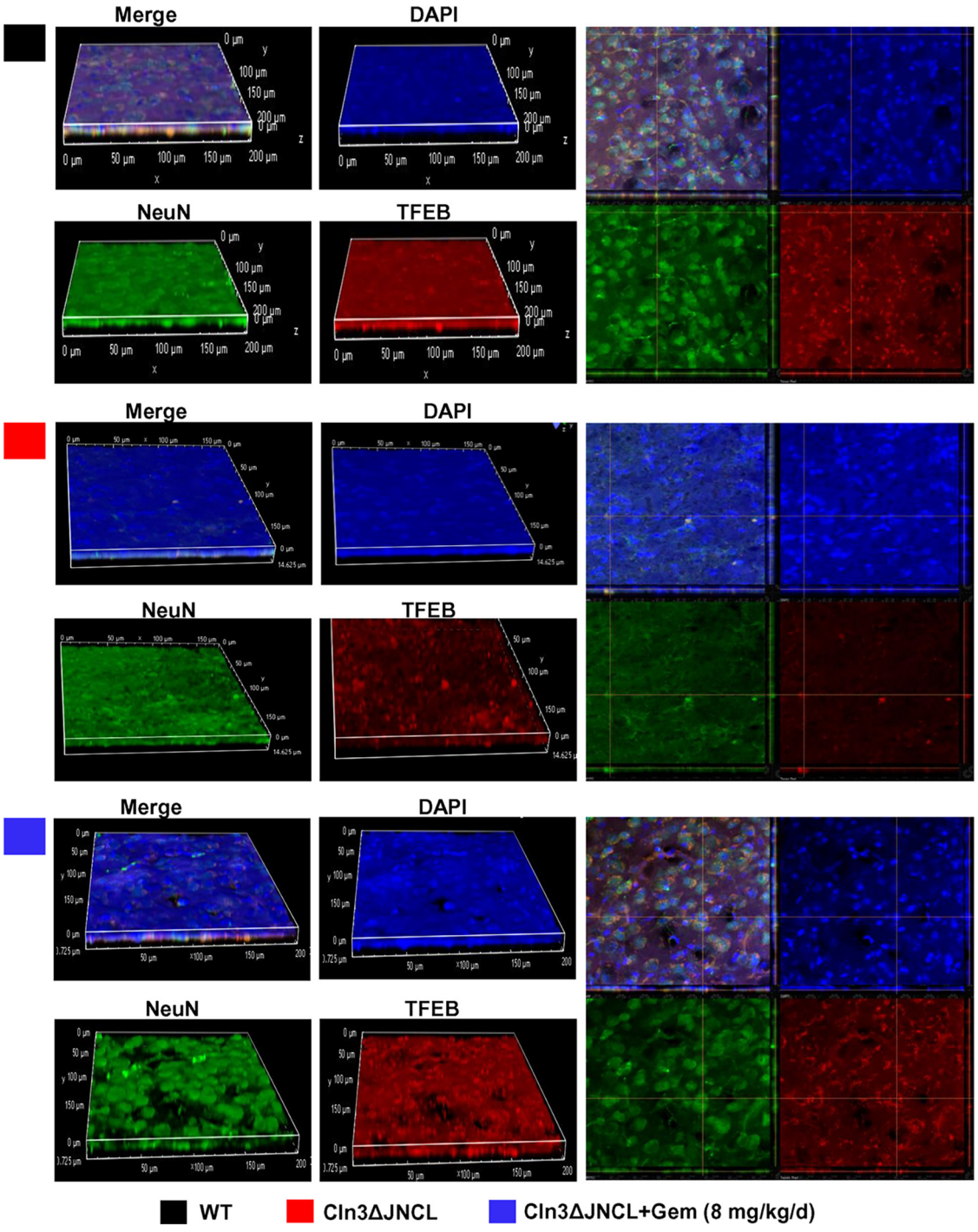

Figure 4. Confocal imaging with three-dimensional volume analysis of TFEB in the SBF cortex of Cln3ΔJNCL mice. Three-month-old Cln3ΔJNCL mice ($n = 6$ per group) of both sexes at equal ratio were treated with gemfibrozil (8 mg/kg body weight) daily via gavage for 3 months. SBF cortical sections were double labeled with antibodies against TFEB and NeuN followed by three-dimensional volume analysis in a Nikon A1 confocal microscope. Results represent analysis of one section of each of six mice per group.

analysis of SBF cortex of Cln3ΔJNCL mice also exhibited a morphologic characteristic of reactive astrogliosis with intense GFAP immunoreactivity (Fig. 1*D*). The number of activated astrocytes/mm^2 was also significantly higher in Cln3ΔJNCL mice than in WT mice (Fig. 1*F*). However, gemfibrozil treatment markedly inhibited astrogliosis in the SBF cortex of Cln3ΔJNCL mice (Fig. 1*D*,*F*).

Similarly, we next studied the effect of gemfibrozil on microgliosis in Cln3ΔJNCL mice. Reactive microglia have been key contributors in several neurodegenerative disorders including JNCL. Centa et al. (2020) have demonstrated evidence of early microglial activation that predicts regions where neuronal loss occurs later in the disease process in a mouse model of JNCL. Western blot analysis showed that the Iba1 protein level was markedly enhanced in the SBF cortex of Cln3ΔJNCL mice compared with WT mice and that gemfibrozil treatment normalized the level of Iba1 in Cln3ΔJNCL mice (Fig. 1*A*,*C*). WT animals exhibited very little Iba1 protein via immunoblot because to prevent the saturation of Iba-1 bands in SBF cortex of Cln3ΔJNCL mice, the blot was scanned at a very low intensity in a Li-Cor

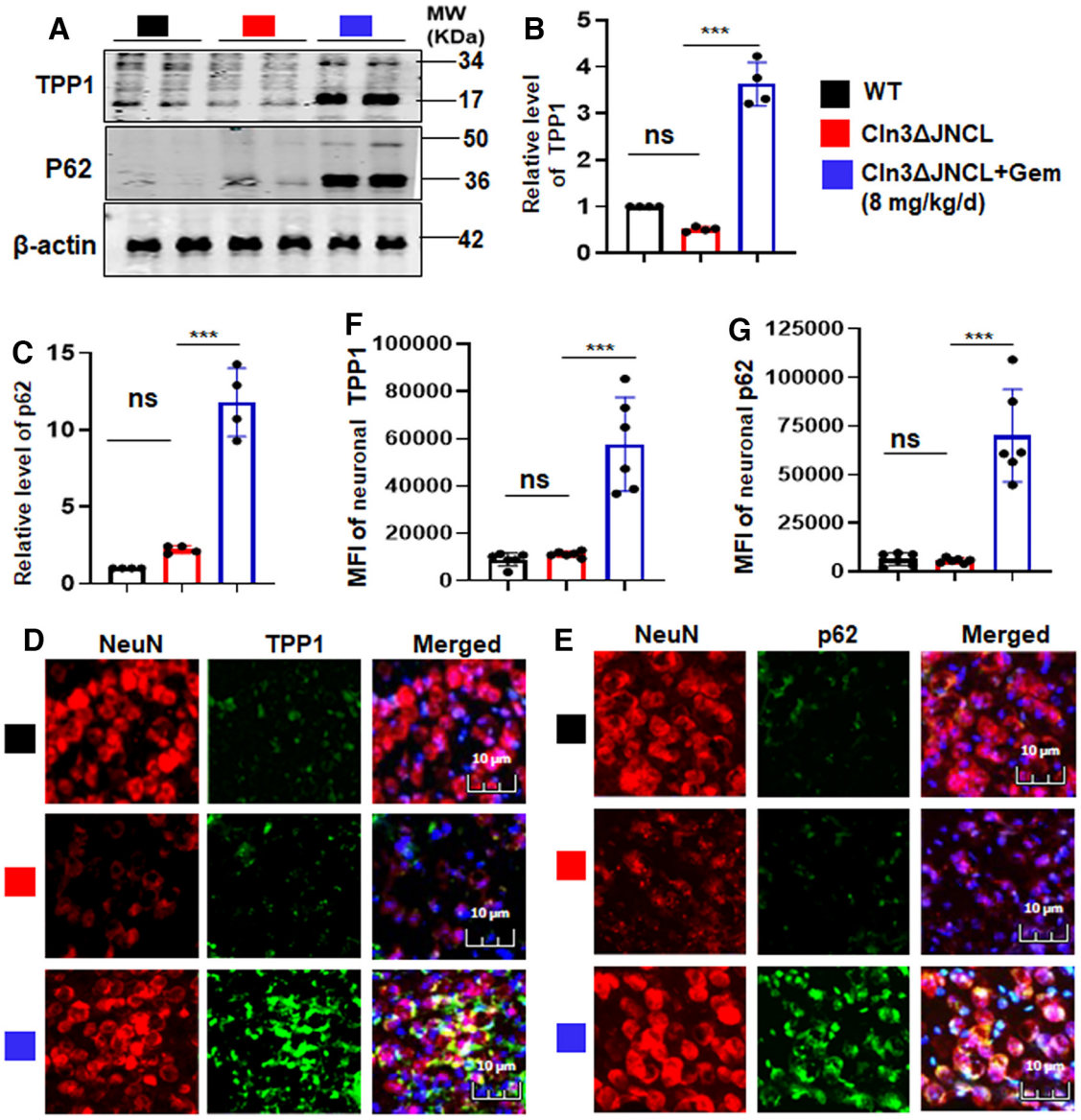

Figure 5. Effect of gemfibrozil on the autophagy pathway in the SBF cortex of Cln3ΔJNCL mice. ***A***, Three-month-old Cln3ΔJNCL mice ($n = 6$ per group) of both sexes at equal ratio were treated with gemfibrozil (8 mg/kg body weight) daily via gavage for 3 months followed by monitoring the level of TPP1 and p62 by Western blot. Actin was run as a loading control. Bands were scanned and values (TPP1/actin, ***B***; p62/Actin, ***C***) presented as relative to WT-control. Results are mean ± SEM of four mice per group. SBF cortical sections were double labeled with antibodies against NeuN and TPP1 (***D***) and NeuN & p62 (***E***). ***F***, ***G***, MFI of TPP1 (***F***) and p62 (***G***) was quantified in two different sections (2 images per section) of each of six different mice ($n = 6$) per group using NIH ImageJ software; $^{***}p < 0.001$. ns, Not significant.

Odyssey Scanner. If we had scanned at a higher intensity, we would have seen nice Iba-1 bands in WT animals. However, at that condition, Iba-1 bands in Cln3ΔJNCL animals would have been oversaturated. Therefore, the Iba-1 Western blot was relative to keeping Iba-1 bands in Cln3ΔJNCL mice in a measurable level; Iba-1 bands in WT mice were low to undetectable. We also performed immunohistochemistry with antibodies against Iba1 and found normal-appearing microglia in WT mice but reactive ones in Cln3ΔJNCL mice (Fig. 1*E*,*G*). However, oral gemfibrozil treatment inhibited microglial activation and decreased the number of activated microglia in the SBF cortex of Cln3ΔJNCL mice (Fig. 1*E*,*G*).

Suppression of proinflammatory molecules in the SBF cortex of Cln3ΔJNCL mice by oral gemfibrozil

Several reports indicate that proinflammatory gene expression is increased in the SBF cortex of Cln3ΔJNCL mice compared with WT mice (Xiong and Kielian, 2013; Dannhausen et al., 2018). Because activated glial cells produce different proinflammatory molecules, and gemfibrozil treatment inhibited glial activation, we investigated the status of different proinflammatory molecules in gemfibrozil-treated and untreated Cln3ΔJNCL mice. Western blot analysis of SBF cortical tissues showed a significant increase in protein levels of inducible nitric oxide synthase (iNOS), pro-IL-1β, IL-1β, and TNFα in Cln3ΔJNCL mice compared with wild-type mice (Fig. 2*A*–*E*). However, consistent with the inhibition of gliosis, gemfibrozil treatment decreased the levels of iNOS, pro-IL-1β, IL-1β, and TNFα in the SBF cortex of Cln3ΔJNCL mice (Fig. 2*A*–*E*). This effect was more prominent at the higher dose (8 mg/kg body weight/d) of gemfibrozil (Fig. 2*A*–*E*). Moreover, the expression of the nitrosative stress marker iNOS was upregulated in GFAP-positive astrocytes and Iba1-positive microglia in SBF cortex of Cln3ΔJNCL mice, which was strongly inhibited by gemfibrozil treatment (Fig. 2*F*,*G*).

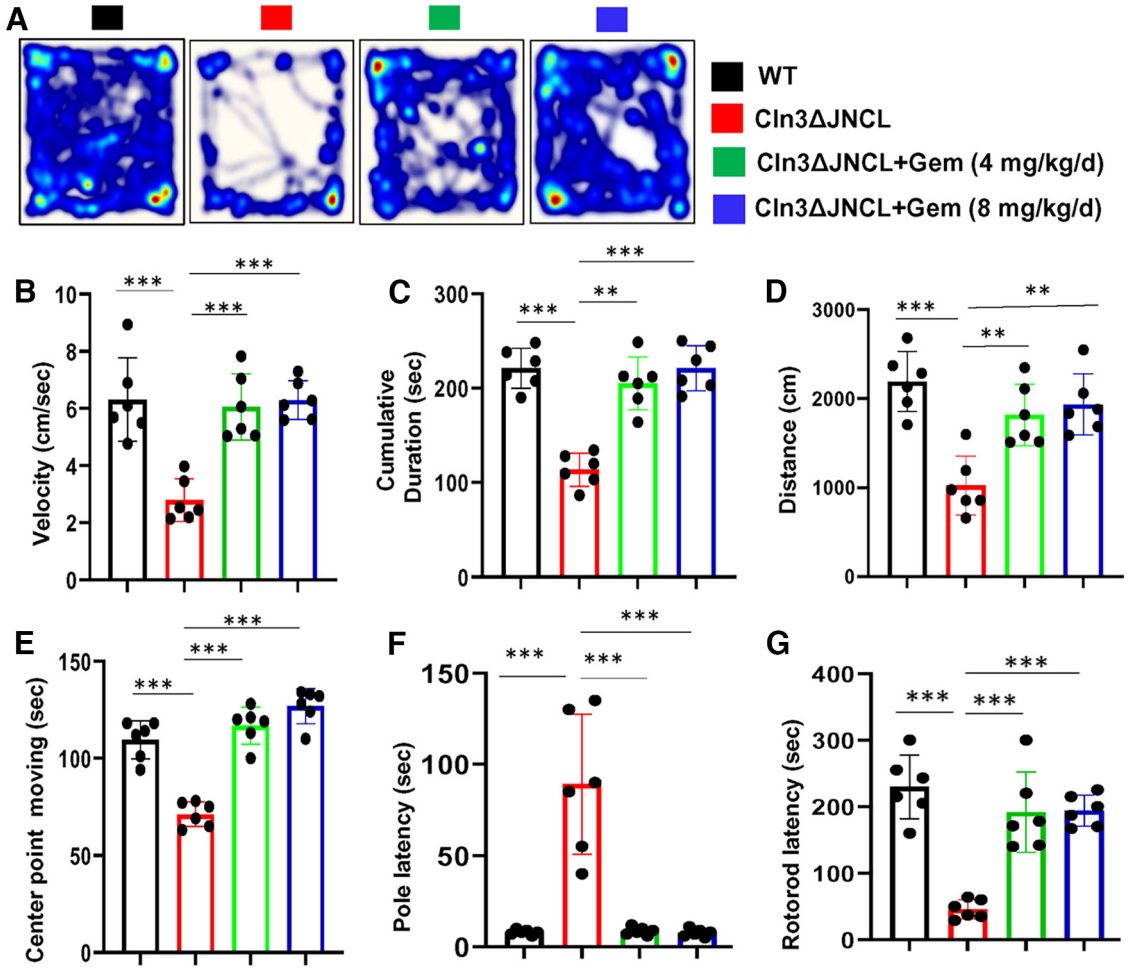

Figure 6. Effect of gemfibrozil on locomotor activities of Cln3ΔJNCL mice. Three-month-old Cln3ΔJNCL mice ($n = 6$ per group) of both sexes at equal ratio were treated with different doses of gemfibrozil (4 and 8 mg/kg body weight) daily via gavage. After 3 months of treatment, open field behavior was monitored by Noldus tracking software. ***A***, Heat map. ***B***, Velocity. ***C***, Cumulative distance. ***D***, Distance moved. ***E***, Center point moving. ***F***, Pole latency. ***G***, Rotarod latency. Results are mean ± SEM of six mice per group; $^{**}p < 0.01$; $^{***}p < 0.001$.

Oral gemfibrozil upregulates TFEB and lowers the burden of storage material in SBF cortex of Cln3ΔJNCL mice

Accumulation of autofluorescent storage material and activation of glia are early neuropathological hallmarks of CLN3 Batten disease that are reciprocated in Cln3ΔJNCL mice (Palmer, 2015). Several studies have demonstrated that TFEB, a master regulator of lysosomal biogenesis, plays a critical role in cellular clearance in neurodegenerative storage diseases (Ghosh et al., 2015; Martini-Stoica et al., 2016; Chandra et al., 2018; Raha et al., 2021). Double-label immunofluorescence analysis of SBF cortical sections for TFEB and NeuN revealed marked decrease in both TFEB (Fig. 3*A*,*B*) and NeuN (Fig. 3*A*,*C*) in 6-month-old Cln3ΔJNCL mice compared with age-matched WT mice. On the other hand, gemfibrozil treatment increased and/or normalized the level of both TFEB (Fig. 3*A*,*B*) and NeuN (Fig. 3*A*,*C*) in the SBF cortex of Cln3ΔJNCL mice. Western blot of SBF cortical tissues for TFEB also corroborates this finding (Fig. 3*D*,*E*). TFEB in SBF cortical sections of either WT mice or gemfibrozil-treated Cln3ΔJNCL mice was present in both cytoplasm and nucleus (Fig. 3*A*). This result was also confirmed by three-dimensional volume analysis in a Nikon A1 confocal microscope (Fig. 4).

TFEB is a transcription factor, and its target genes are ultimately involved in lysosomal biogenesis and autophagy (Ghosh and Pahan, 2016; Napolitano and Ballabio, 2016). Therefore, to confirm the activation of TFEB, we monitored the status of tripeptidyl-peptidase 1 (TPP1) and p62, molecules that are controlled by TFEB, in the SBF cortex of Cln3ΔJNCL mice. As evident from Western blot analysis, gemfibrozil treatment markedly increased the level of both TPP1 (Fig. 5*A*,*B*) and p62 (Fig. 5*A*,*C*) in the SBF cortex of Cln3ΔJNCL mice. To confirm this finding further, we performed double-label immunofluorescence analysis that also exhibited a marked increase in both TPP1 (Fig. 5*D*, *F*) and p62 (Fig. 5*E*,*G*) in the SBF cortex of Cln3ΔJNCL mice on gemfibrozil treatment. These results suggest that gemfibrozil treatment is capable of stimulating the activated form of TFEB and that gemfibrozil increases autophagy in the CNS of Cln3ΔJNCL mice.

Next, we investigated whether gemfibrozil treatment could reduce the level of autofluorescent storage material containing SCMAS in SBF cortex of Cln3ΔJNCL mice. Expectedly, we found striking accumulation of SCMAS in the SBF cortex of Cln3ΔJNCL mice compared with WT mice (Fig. 3*F*,*G*). Yet consistent with the upregulation of TFEB, gemfibrozil treatment steered to a striking decrease in SCMAS in the SBF cortex of Cln3ΔJNCL mice (Fig. 3*F*,*G*).

Oral gemfibrozil improves locomotor activities in Cln3ΔJNCL mice

Decreasing functional impairment is definitely a therapeutic goal of neuroprotection for JNCL patients. Similar to that observed in

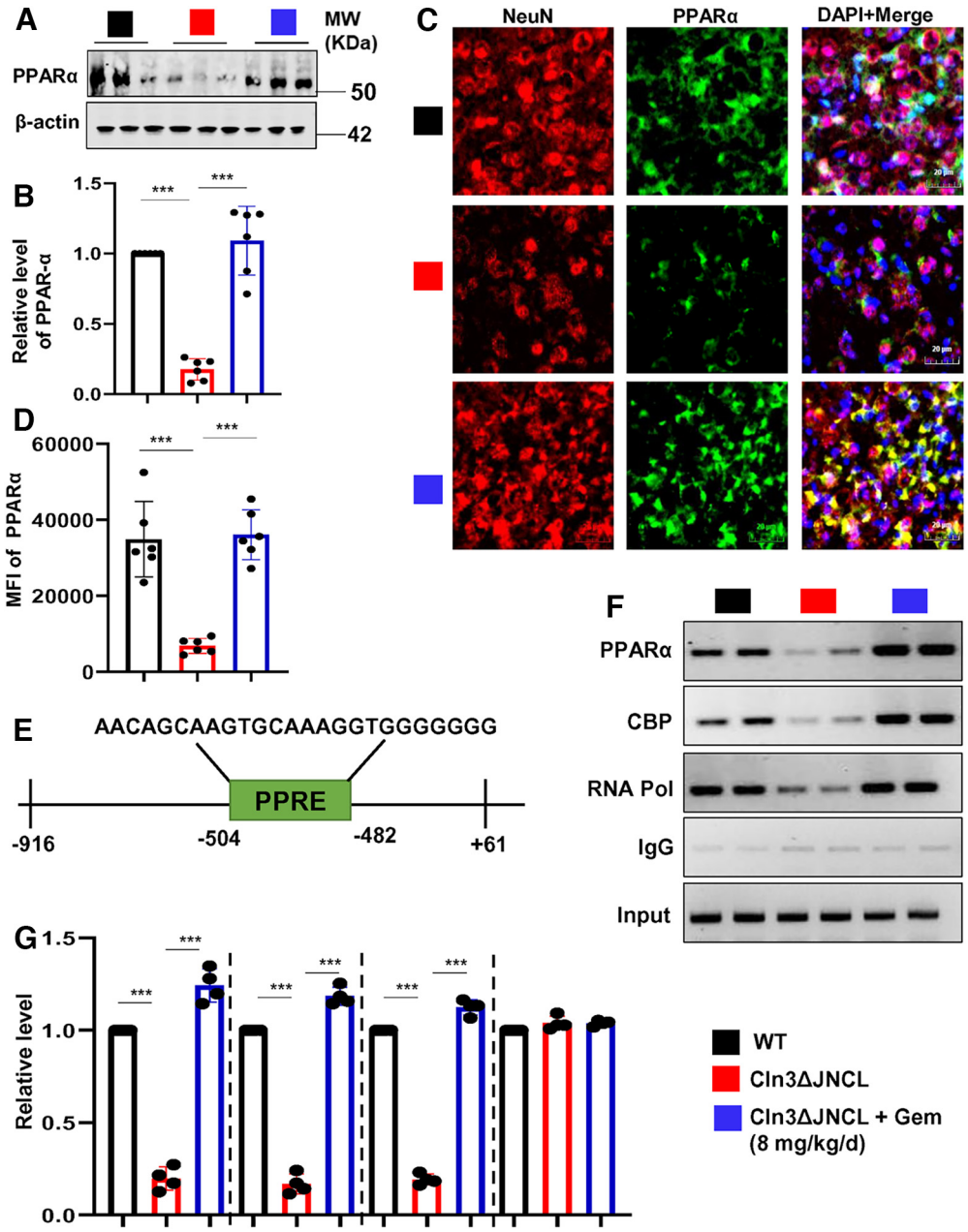

Figure 7. Oral administration of gemfibrozil increases the level of PPARα and the recruitment of PPARα to *Tfeb* promoter in the SBF cortex of Cln3ΔJNCL mice. ***A***, Three-month-old Cln3ΔJNCL mice ($n = 6$ per group) of both sexes at equal ratio were treated with gemfibrozil (8 mg/kg body weight) daily via gavage for 3 months followed by monitoring the protein level of PPARα by Western blot. ***B***, Bands were scanned and values (PPARα/actin) presented as relative to WT-control. ***C***, Immunostaining of SBF cortical sections for PPARα and NeuN. ***D***, MFI of PPARα was quantified in two different sections (2 images per section) of each of six different mice ($n = 6$) per group using NIH ImageJ software. ***E***, Schematic representation of the mouse *Tfeb* gene promoter with PPRE. ***F***, ***G***, *In situ* ChIP for PPARα, CBP, and RNA-polymerase followed by semiquantitative (***F***) and quantitative PCR (***G***) analyses performed in SBF cortex; $^{***}p < 0.001$.

JNCL patients, Cln3ΔJNCL mice also exhibit motor deficits (Kovács and Pearce, 2008). Therefore, locomotor activities were checked in gemfibrozil-treated and untreated 6-month-old Cln3ΔJNCL mice. As expected, Cln3ΔJNCL mice displayed a decrease in horizontal activity (Fig. 6*A*), velocity (Fig. 6*B*), cumulative duration (Fig. 6*C*), total distance traveled (Fig. 6*D*), and center point moving (Fig. 6*E*) compared with age-matched WT mice. In the pole test, WT mice climbed down the pole quickly and touched the base of the pole without hesitation, whereas Cln3ΔJNCL mice showed abnormal behavior, which included turning upward, falling off the pole, slowly descending, freezing on the pole, and hesitating to touch the base of the pole (Fig. 6*F*). Similarly as evident from rotorod latency (Fig. 6*G*), Cln3ΔJNCL mice performed very poorly on the rotorod, affirming the compromised motor coordination and muscle strength experience by these animals. However, oral administration of gemfibrozil significantly improved open field, pole, and rotorod activities of Cln3ΔJNCL mice (Fig. 6), showing improved locomotor performance of Cln3ΔJNCL mice by gemfibrozil. Therefore, it can be surmised that reduction of Batten pathology positively correlates with improved motor functions in gemfibrozil-treated Cln3ΔJNCL mice.

Oral administration of gemfibrozil stimulates the recruitment of PPARα to the *tfeb* gene promoter in SBF cortex of Cln3ΔJNCL mice

Next, we investigated the mechanism by which gemfibrozil upregulated TFEB to prevent the accumulation of storage materials

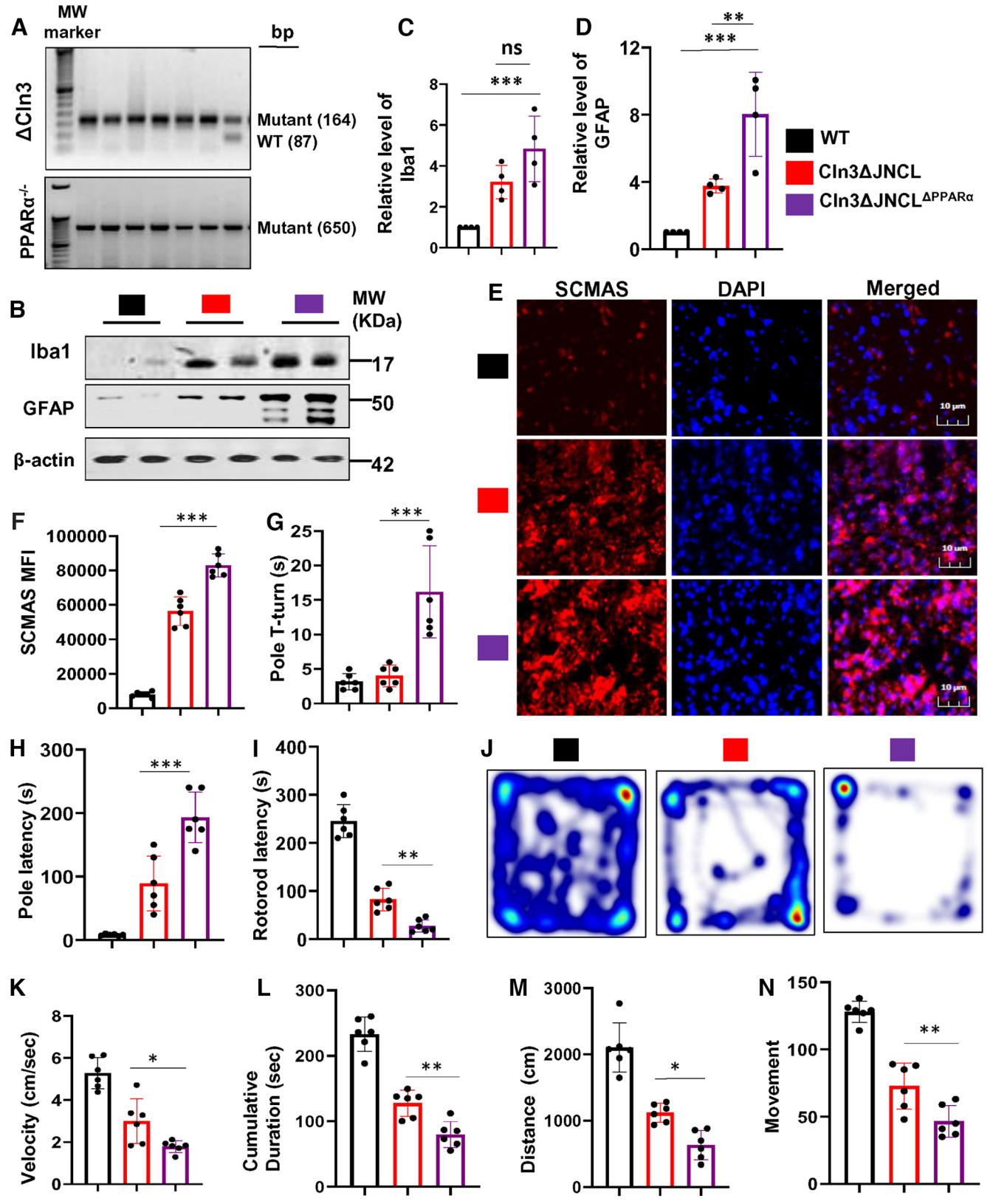

Figure 8. Deletion of PPARα aggravates the disease process in Cln3ΔJNCL mice. ***A***, Genetic screening of Cln3ΔJNCL mice lacking PPARα (Cln3ΔJNCL$^{\Delta PPAR\alpha}$). ***B***, Three-month-old Cln3ΔJNCL and Cln3ΔJNCL$^{\Delta PPAR\alpha}$ mice ($n = 6$ per group) of both sexes at equal ratio were treated with gemfibrozil (8 mg/kg body weight) daily via gavage for 3 months followed by monitoring the protein level of Iba-1 and GFAP by Western blot. ***C***, ***D***, Bands were scanned and values (cytokine/actin) presented as relative to WT-control (***C***, Iba1; ***D***, GFAP). ***E***, Immunostaining of SBF cortical sections for SCMAS. ***F***, MFI of SCMAS was quantified in two different sections (2 images per section) of each of six different mice ($n = 6$) per group using NIH ImageJ software. ***G–N***, Mice were monitored for pole test (***G***, pole T-turn; ***H***, pole latency), rotorod test (***I***), and open field behavior (***J***, heat map; ***K***, velocity; ***L***, cumulative duration; ***M***, distance traveled; ***N***, movement). Results are mean ± SEM of six mice per group; *$p < 0.05$; **$p < 0.01$; ***$p < 0.001$.

in Cln3ΔJNCL mice. As gemfibrozil is known to activate PPARα (Lovett-Racke et al., 2004; Roy and Pahan, 2009; Ghosh et al., 2012; 2015; Ghosh and Pahan, 2016), we examined the role of PPARα. Western blot results showed that the protein level of PPARα markedly decreased in the SBF cortex of Cln3ΔJNCL mice compared with wild-type mice (Fig. 7*A*,*B*). On the other hand, gemfibrozil treatment significantly increased and/or restored the PPARα level in the CNS of Cln3ΔJNCL mice (Fig. 7*A*,*B*). Double-label immunofluorescence of cortical sections of gemfibrozil-treated and untreated Cln3ΔJNCL mice for NeuN and PPARα also validates this finding (Fig. 7*C*,*D*).

We have demonstrated that activation of PPARα transcriptionally upregulates *Tfeb* and stimulates lysosomal biogenesis in brain cells (Ghosh et al., 2015; Ghosh and Pahan, 2016; Chandra et al., 2018). Therefore, by using *in situ* ChIP we investigated whether oral gemfibrozil treatment stimulated the recruitment of PPARα to the *Tfeb* gene promoter *in vivo* in the SBF cortex of Cln3ΔJNCL mice. Figure 7*E* indicates the presence of a consensus PPRE in *Tfeb* gene promoter. After immunoprecipitation of chromatin fragments by antibodies against PPARα, we were able to amplify a 200 bp fragment encompassing the PPRE of the *Tfeb* promoter in SBF cortex of WT, but not Cln3ΔJNCL, mice (Fig. 7*F*,*G*), indicating decreased enrolment of PPARα to the *Tfeb* gene promoter in the CNS of Cln3ΔJNCL mice. However, gemfibrozil treatment markedly restored/increased the recruitment of PPARα to the *Tfeb* gene promoter in the SBF cortex of Cln3ΔJNCL mice (Fig. 7*F*,*G*). Similarly, we also observed decreased employment of CBP, an important histone acetyl transferase, and RNA polymerase in the *Tfeb* promoter in the CNS of ΔCln3 mice, which was restored by gemfibrozil treatment (Fig. 7*F*,*G*). These results are specific as no product amplification was observed in immunoprecipitants with control IgG. Together, these results indicate that oral gemfibrozil stimulates the recruitment of PPARα to the *Tfeb* promoter *in vivo* in the CNS of Cln3ΔJNCL mice.

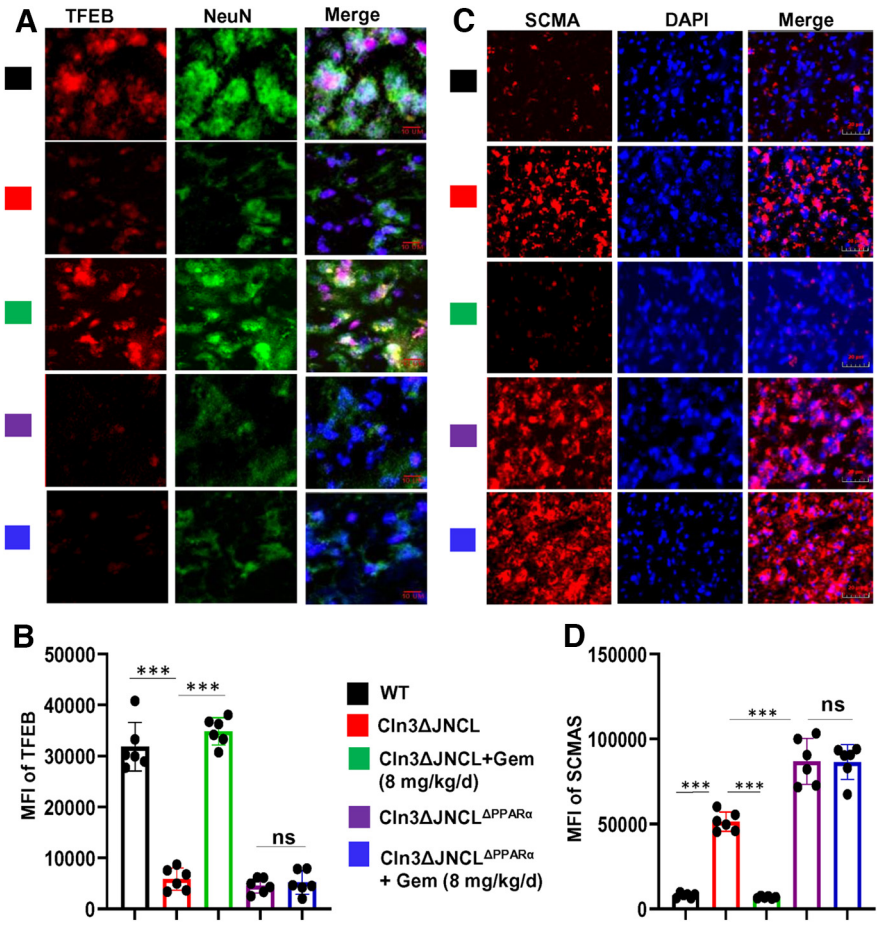

Figure 9. Effect of gemfibrozil on the level of TFEB and storage materials in the SBF cortex of Cln3ΔJNCL and Cln3ΔJNCL$^{\Delta PPAR\alpha}$ mice. Three-month-old Cln3ΔJNCL and Cln3ΔJNCL$^{\Delta PPAR\alpha}$ mice ($n = 6$ per group) of both sexes at equal ratio were treated with gemfibrozil (8 mg/kg body weight) daily via gavage for 3 months followed by double labeling of SBF cortical sections for NeuN and TFEB. ***A***, Images were obtained with 20× magnification in Nikon A1 confocal microscope. ***B***, MFI of TFEB was quantified in two different sections (2 images per section) of each of six different mice ($n = 6$) per group using NIH ImageJ software. ***C***, SBF cortical sections were also immunostained with antibodies against SCMAS. DAPI was used to visualize nucleus. ***D***, MFI of SCMAS was quantified in two different sections (2 images per section) of each of six different mice ($n = 6$) per group using NIH ImageJ software. Results are mean ± SEM of six mice per group; ***$p < 0.001$; ns, Not significant.

Knockdown of PPARα aggravates JNCL pathologies and worsens locomotor performance in Cln3ΔJNCL mice

To further reveal the role of PPARα in JNCL pathologies, we crossed Cln3ΔJNCL mice with PPARα$^{-/-}$ mice to generate Cln3ΔJNCL$^{\Delta PPAR\alpha}$ mice (Fig. 8*A*). Interestingly, deletion of PPARα from Cln3ΔJNCL mice increased glial activation in the SBF cortex as evident from upregulation of Iba-1 and GFAP (Fig. 8*B*–*D*). Immunofluorescence analysis also demonstrated increased accumulation of SCMAS in the SBF cortex of Cln3ΔJNCL$^{\Delta PPAR\alpha}$ mice compared with Cln3ΔJNCL mice (Fig. 8*E*,*F*).

Next, we compared locomotor activities between Cln3ΔJNCL and Cln3ΔJNCL$^{\Delta PPAR\alpha}$ mice. As evident from the pole test, Cln3ΔJNCL$^{\Delta PPAR\alpha}$ mice took a longer time to make the T turn (Fig. 8*G*) and descend the vertical pole (Fig. 8*H*) compared with Cln3ΔJNCL mice. Similarly, Cln3ΔJNCL$^{\Delta PPAR\alpha}$ mice exhibited poor performance on the rotorod compared with Cln3ΔJNCL mice (Fig. 8*I*). Consistently, Cln3ΔJNCL mice were more efficient than Cln3ΔJNCL$^{\Delta PPAR\alpha}$ mice in overall locomotor activities (Fig. 8*J*), velocity (Fig. 8*K*), cumulative duration (Fig. 8*L*), distance traveled (Fig. 8*M*), and movement (Fig. 8*N*). These results suggest that PPARα may play an important role in JNCL.

Oral gemfibrozil upregulates TFEB, decreases storage materials, and reduces glial activation in the SBF cortex of Cln3ΔJNCL mice via PPARα

To confirm that gemfibrozil does in fact require PPARα to exert its neuroprotective effects in Cln3ΔJNCL mice, we monitored the level of TFEB and the buildup of storage material SCMAS in SBF cortex of gemfibrozil-treated Cln3ΔJNCL mice and Cln3ΔJNCL$^{\Delta PPAR\alpha}$ mice. In contrast to the upregulation of TFEB and the reduction of storage materials in Cln3ΔJNCL mice, gemfibrozil treatment remained unable to increase TFEB

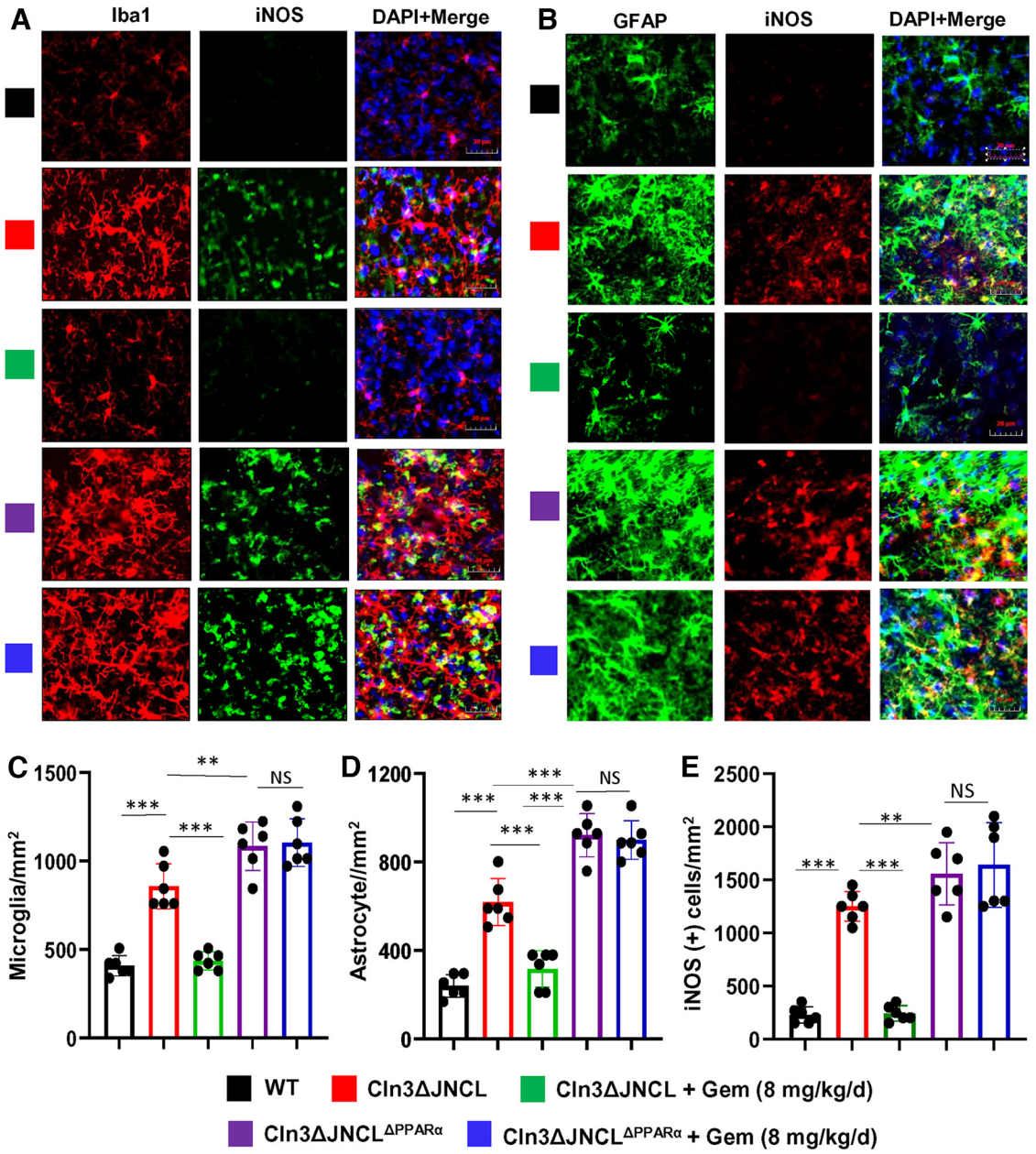

Figure 10. Effect of gemfibrozil on glial activation in the SBF cortex of Cln3ΔJNCL and Cln3ΔJNCL$^{\Delta PPAR\alpha}$ mice. Three-month-old Cln3ΔJNCL and Cln3ΔJNCL$^{\Delta PPAR\alpha}$ mice ($n = 6$ per group) of both sexes at equal ratio were treated with gemfibrozil (8 mg/kg body weight) daily via gavage. ***A***, ***B***, After 3 months of treatment, mice were perfused, and SBF cortical sections were double labeled for Iba1 and iNOS (***A***) and GFAP and iNOS (***B***). ***C–E***, DAPI was used to visualize nucleus. Iba1-positive (***C***), GFAP-positive (***D***), and iNOS-positive (***E***) cells were counted in one section (2 images per section) of each of six different mice ($n = 6$) per group. Results represent analysis of one section of each of six different mice per group; $^{***}p < 0.001$.

(Fig. 9*A*,*B*) and decrease storage materials (Fig. 9*C*,*D*) in Cln3ΔJNCL$^{\Delta PPAR\alpha}$ mice. Neuronal loss is seen in Cln3ΔJNCL mice, and although gemfibrozil protected NeuN-positive neurons in Cln3ΔJNCL mice (Figs. 3*A*,*C*, 9*A*), such neuronal protection was not seen by gemfibrozil in Cln3ΔJNCL$^{\Delta PPAR\alpha}$ mice (Fig. 9*A*). These results suggest that gemfibrozil involves PPARα for the upregulation of TFEB, reduction of storage materials, and the protection of neurons in the CNS of Cln3ΔJNCL mice.

Next, we examined whether gemfibrozil entails PPARα to reduce glial activation in the CNS of Cln3ΔJNCL mice. Although at a dose of 8 mg/kg body weight/d, gemfibrozil markedly decreased the activation of microglia (Fig. 10*A*,*C*) and astroglia (Fig. 10*B*,*D*) and reduced the level of iNOS (Fig. 10*A*,*B*,*E*) in the SBF cortex of Cln3ΔJNCL mice, we did not find any inhibition of glial activation and drop in iNOS expression by gemfibrozil in Cln3ΔJNCL$^{\Delta PPAR\alpha}$ mice, suggesting that oral gemfibrozil is also unable to suppress glial inflammation in the absence of PPARα.

Gemfibrozil improves locomotor activities in Cln3ΔJNCL mice via PPARα

Because gemfibrozil treatment recovered locomotor activities in Cln3ΔJNCL mice (Fig. 6), we investigated whether such protection was also dependent on PPARα. Therefore, Cln3ΔJNCL$^{\Delta PPAR\alpha}$ mice were treated with gemfibrozil orally for 3 months followed by monitoring open field activities and pole test and rotorod performance. Consistent with the failure of gemfibrozil to reduce the accumulation of SCMAS and

inhibit glial activation, gemfibrozil, in this instance as well, remained unable to improve overall open field performance (Fig. 11*A*), velocity (Fig. 11*B*), cumulative duration (Fig. 11*C*), distance traveled (Fig. 11*D*), and center point moving (Fig. 11*E*) of Cln3ΔJNCL$^{\Delta PPAR\alpha}$ mice. Accordingly, gemfibrozil also did not improve the performance of Cln3ΔJNCL$^{\Delta PPAR\alpha}$ mice on a moving rotorod (Fig. 11*F*) and on pole descending (Fig. 11*G*,*H*), indicating that gemfibrozil enhances locomotor activities of Cln3ΔJNCL mice via PPARα.

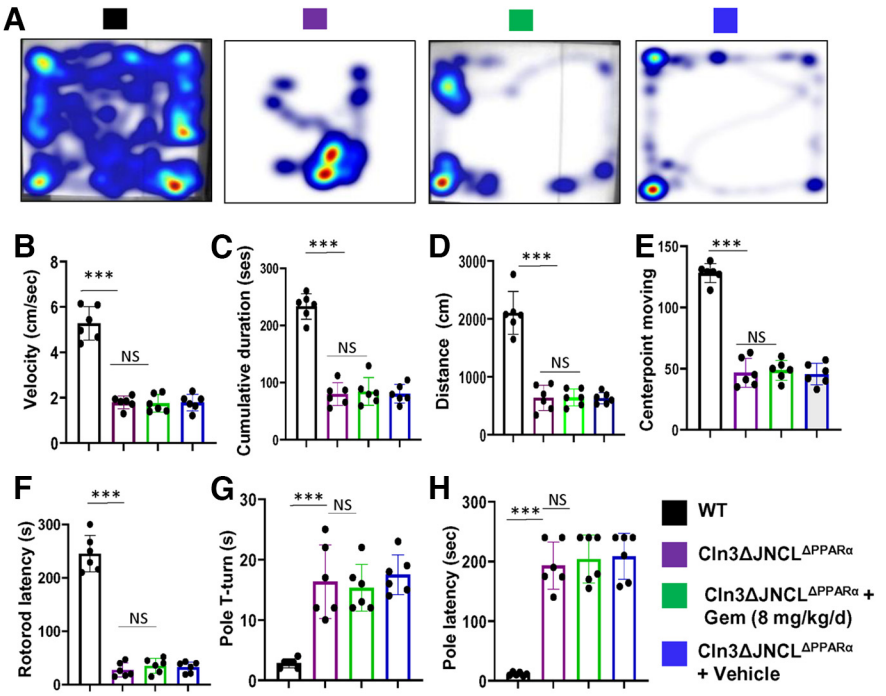

Figure 11. Effect of gemfibrozil on locomotor activities of Cln3ΔJNCL$^{\Delta PPAR\alpha}$ mice. Three-month-old Cln3ΔJNCL$^{\Delta PPAR\alpha}$ mice ($n = 6$ per group) of both sexes at equal ratio were treated with gemfibrozil (8 mg/kg body weight) daily via gavage. ***A–H***, After 3 months of treatment, locomotor activities were monitored by open-field behavior (***A***, heat map; ***B***, velocity; ***C***, cumulative duration; ***D***, distance traveled; ***E***, center point moving), rotorod performance (***F***), and pole test (***G***, pole T-turn; ***H***, pole latency). Results are mean ± SEM of six mice per group; ***$p < 0.001$; ns, not significant.

Discussion

The NCLs or Batten disease are a group of recessively inherited fatal lysosomal storage disorders of infants, with rare adult forms (Kim et al., 2017; Johnson et al., 2019). Each form of NCL is caused by mutations in a different gene, which determine the age of disease onset, symptoms, and rate of disease progression, but all are fatal after a period of prolonged disability. Other than Brineura therapy for late infantile NCL (LINCL), there are no effective therapies for NCL. Different therapeutic approaches (e.g., enzyme replacement, immunosuppression, cell therapy, and gene therapy) are being considered for delaying or halting the progression of these devastating rare diseases (Kim et al., 2017; Johnson et al., 2019). However, the transmembrane protein CLN3 is not secreted like either CLN1 or CLN2, and therefore there is no option of its uptake by neighboring cells (Johnson et al., 2019). Furthermore, as the disease process of JNCL is widespread in different parts of the brain, on intracranial delivery, recombinant functional proteins or viral vectors may not reach the appropriate target cell type overcoming the densely populated cells (Mole and Cotman, 2015; Kim et al., 2017; Johnson et al., 2019). Although gene therapy trials are ongoing, development of neuroprotective therapeutic approaches for delaying the disease progression, improving locomotor functions, and increasing the survival of JNCL patients are of paramount importance. Cln3$^{\Delta ex7/8}$ (Cln3ΔJNCL) mice are useful in determining new therapeutic strategies and testing the efficacy of new drugs for JNCL. Here, we demonstrate for the first time that oral administration of gemfibrozil, an FDA-approved drug for hyperlipidemia in humans, reduces the CNS accumulation of storage material, decreases glial activation, and improves locomotor functions in Cln3ΔJNCL mice. Because of the increase in proinflammatory molecules in the CNS of ΔCln3 mice, there is the possibility that the motor impairments observed are because of sickness behavior, not structural alterations in the CNS. Although gemfibrozil treatment lowers the load of storage materials and improves the status of neurons as monitored by an increase in NeuN, further studies are needed to confirm that gemfibrozil-mediated improvement in locomotor performance in Cln3ΔJNCL mice is not because of suppression of neuroinflammation. Nevertheless, these results suggest that oral gemfibrozil may be beneficial for JNCL patients.

Accumulation of lipophilic and ceroid-like autofluorescent storage material in both neurons and non-neuronal cells is a signature feature of NCLs including JNCL. Mechanisms leading to the clearance of storage materials are becoming clear. Autophagy is the way the cell removes unnecessary or dysfunctional components through a lysosome-dependent degradation process to maintain cell homeostasis. Because aberrant lysosomal function and autophagy have been associated with multiple lysosomal storage and neurodegenerative disorders, upregulation of this lysosome–autophagy pathway has emerged as an attractive therapeutic strategy. TFEB is known as a master regulator of lysosomal biogenesis, and several studies have shown that TFEB overexpression is capable of alleviating neurodegenerative pathology through upregulation of the autophagy–lysosome pathway (Wang et al., 2016; Becot et al., 2020). Recently, we have taken a different approach to upregulate TFEB. We have demonstrated that the *Tfeb* gene promoter harbors a consensus PPRE and that activation of PPARα, neither PPARβ nor PPARγ, leads to transcriptional upregulation of *Tfeb* (Ghosh et al., 2015; Ghosh and Pahan, 2016; Chandra et al., 2018). Because gemfibrozil is a known agonist of PPARα, we examined the role of this molecule and found that gemfibrozil treatment reduced CNS deposition of autofluorescent storage materials and exhibited neuroprotective effects via PPARα. Our conclusion is based on the following: First, the PPARα level was low in the SBF cortex of 6-month-old Cln3ΔJNCL mice as compared with age-matched WT mice, which was increased and/or normalized by oral gemfibrozil. Second, the JNCL disease process decreased the recruitment of PPARα to the *Tfeb* gene promoter as we found decreased enrollment of PPARα to *Tfeb* promoter in the SBF cortex of Cln3ΔJNCL mice in

comparison with WT mice. However, gemfibrozil treatment was capable of stimulating PPARα recruitment to the *Tfeb* promoter *in vivo* in the CNS of Cln3ΔJNCL mice. Third, the level of TFEB also decreased in the CNS of Cln3ΔJNCL mice that was increased by gemfibrozil treatment. Fourth, gemfibrozil was unable to decrease storage materials and improve locomotor performance in Cln3ΔJNCL mice lacking PPARα.

Similar to that found in other neurodegenerative disorders, activation of astrocytes and microglia is an early pathologic event in human JNCL (Haltia et al., 2001; Tyynelä et al., 2004; Johnson et al., 2019) as well as in the Cln3ΔJNCL mouse model of JNCL (Pontikis et al., 2005; Sun, 2018). Early-onset microgliosis has also been reported to closely accompany light-induced retinal degeneration in Cln3ΔJNCL mice and the progressive loss of photoreceptor cells in the *nclf* mouse model of CLN6 disease (Dannhausen et al., 2018; Atiskova et al., 2019). Here, we also found upregulation of GFAP and Iba-1 and associated expression of IL-1β, TNFα, and iNOS in SBF cortex of Cln3ΔJNCL mice. However, consistent with inhibition of proinflammatory molecules in cultured astrocytes and microglia (Pahan et al., 2002; Jana et al., 2007), oral gemfibrozil treatment suppressed glial activation and inflammation in Cln3ΔJNCL mice. However, gemfibrozil did not inhibit glial inflammation in Cln3ΔJNCL mice lacking PPARα, indicating an essential role of PPARα in this process. Suppressor of cytokine signaling (SOCS) proteins also play a crucial role in inhibiting cytokine signaling and inflammatory gene expression in various cell types, including glial cells (Baker et al., 2009; Ghosh et al., 2012; Ghosh and Pahan, 2012). Similarly, IL-1R antagonist (IL-1Ra) inhibits proinflammatory cell signaling by adhering to IL-1R, receptor for IL-1α and IL-1β (Corbett et al., 2012; Malik and Kanneganti, 2018). We have seen that gemfibrozil is capable of upregulating both SOCS3 and IL-1Ra in brain cells (Corbett et al., 2012; Ghosh and Pahan, 2012). Gemfibrozil treatment is also capable of increasing the level of SOCS3 and IL-1Ra in striatum and cortex and exhibiting neuroprotection in *Cln2*$^{(-/-)}$ mice (Ghosh et al., 2017). Recently, we have demonstrated the involvement of PPARα in aspirin-induced transcription of both *SOCS3* and *IL-1Ra* in astrocytes (Chakrabarti et al., 2019, 2021), indicating that gemfibrozil being a prototype agonist of PPARα may also involve PPARα for the upregulation of SOCS3 and IL-1Ra and hence exhibition of anti-inflammation.

Gemfibrozil has several advantages over other prospective neuroprotective agents. For example, gemfibrozil is an oral drug and fairly nontoxic (Pahan et al., 2002; Kim et al., 2017). After oral administration, it can cross the blood–brain barrier (Dasgupta et al., 2007; Corbett et al., 2012). It is neuroprotective and can increase the life span of *Cln2*$^{(-/-)}$ mice, an animal model of LINCL (Ghosh et al., 2017). Gemfibrozil has been reported to be safe for lowering lipids in children (Kim et al., 2017). Although the primary site of CLN3 disease manifestation is the CNS, buildup of lysosomal storage material occurs in different part of the body, and as a result, cardiac abnormality is also observed in children as the disease progresses. In this context, gemfibrozil may be able to prevent cardiac disease in JNCL patients. Moreover, gemfibrozil exhibits neurotrophic (Roy et al., 2007; Gottschalk et al., 2021) and promyelinating effects (Jana et al., 2012) and supports memory and learning (Chandra and Pahan, 2019). However, at present, nothing is known about the level of PPARα in JNCL patients. As gemfibrozil requires PPARα to exhibit neuroprotection in Cln3ΔJNCL mice, in the absence of a basal level of PPARα, gemfibrozil may not exhibit optimal therapeutic efficacy in JNCL patients. Therefore, future studies may be directed to address this aspect.

In summary, this study demonstrates that oral administration of gemfibrozil, an FDA-approved lipid-lowering drug in humans, exhibits neuroprotective effects in an animal model of JNCL. In particular, gemfibrozil reduces storage materials, attenuates glial inflammation, and improves locomotor activities in a mouse model of JNCL via PPARα, suggesting that gemfibrozil may not be neuroprotective for JNCL in the absence of PPARα. Although the *in vivo* state of Cln3ΔJNCL mice does not truly bear a resemblance to the *in vivo* scenario of JNCL patients, and not much is known about the status of PPARα in JNCL, our results suggest that activation of PPARα by oral gemfibrozil may have therapeutic importance in JNCL.

References

Atiskova Y, Bartsch S, Danyukova T, Becker E, Hagel C, Storch S, Bartsch U (2019) Mice deficient in the lysosomal enzyme palmitoyl-protein thioesterase 1 (PPT1) display a complex retinal phenotype. Sci Rep 9:14185.

Baker BJ, Akhtar LN, Benveniste EN (2009) SOCS1 and SOCS3 in the control of CNS immunity. Trends Immunol 30:392–400.

Becot A, Pardossi-Piquard R, Bourgeois A, Duplan E, Xiao Q, Diwan A, Lee JM, Lauritzen I, Checler F (2020) The transcription factor EB reduces the intraneuronal accumulation of the beta-secretase-derived APP fragment C99 in cellular and mouse Alzheimer's disease models. Cells 9:1204.

Bosch ME, Aldrich A, Fallet R, Odvody J, Burkovetskaya M, Schuberth K, Fitzgerald JA, Foust KD, Kielian T (2016) Self-complementary AAV9 gene delivery partially corrects pathology associated with juvenile neuronal ceroid lipofuscinosis (CLN3). J Neurosci 36:9669–9682.

Brenneman DE, Pearce DA, Kovacs A, DeFrees S (2017) Pharmacological effects on ceroid lipofuscin and neuronal structure in Cln3 (ex7/8) mouse brain cultures. J Mol Neurosci 63:100–114.

Cao Y, Espinola JA, Fossale E, Massey AC, Cuervo AM, MacDonald ME, Cotman SL (2006) Autophagy is disrupted in a knock-in mouse model of juvenile neuronal ceroid lipofuscinosis. J Biol Chem 281:20483–20493.

Cao Y, Staropoli JF, Biswas S, Espinola JA, MacDonald ME, Lee JM, Cotman SL (2011) Distinct early molecular responses to mutations causing vLINCL and JNCL presage ATP synthase subunit C accumulation in cerebellar cells. PLoS One 6:e17118.

Centa JL, Jodelka FM, Hinrich AJ, Johnson TB, Ochaba J, Jackson M, Duelli DM, Weimer JM, Rigo F, Hastings ML (2020) Therapeutic efficacy of antisense oligonucleotides in mouse models of CLN3 Batten disease. Nat Med 26:1444–1451.

Chakrabarti S, Roy A, Prorok T, Patel D, Dasarathi S, Pahan K (2019) Aspirin up-regulates suppressor of cytokine signaling 3 in glial cells via PPARα. J Neurochem 151:50–63.

Chakrabarti S, Prorok T, Roy A, Patel D, Dasarathi S, Pahan K (2021) Upregulation of IL-1 receptor antagonist by aspirin in glial cells via peroxisome proliferator-activated receptor-alpha. J Alzheimers Dis Rep 5:647–661.

Chandra G, Rangasamy SB, Roy A, Kordower JH, Pahan K (2016) Neutralization of RANTES and eotaxin prevents the loss of dopaminergic neurons in a mouse model of Parkinson disease. J Biol Chem 291:15267–15281.

Chandra S, Pahan K (2019) Gemfibrozil, a lipid-lowering drug, lowers amyloid plaque pathology and enhances memory in a mouse model of Alzheimer's disease via peroxisome proliferator-activated receptor α. J Alzheimers Dis Rep 3:149–168.

Chandra S, Jana M, Pahan K (2018) Aspirin induces lysosomal biogenesis and attenuates amyloid plaque pathology in a mouse model of Alzheimer's disease via PPARα. J Neurosci 38:6682–6699.

Cooper JD, Tarczyluk MA, Nelvagal HR (2015) Towards a new understanding of NCL pathogenesis. Biochim Biophys Acta 1852:2256–2261.

Corbett GT, Roy A, Pahan K (2012) Gemfibrozil, a lipid-lowering drug, upregulates IL-1 receptor antagonist in mouse cortical neurons: implications for neuronal self-defense. J Immunol 189:1002–1013.

Corbett GT, Gonzalez FJ, Pahan K (2015) Activation of peroxisome proliferator-activated receptor α stimulates ADAM10-mediated proteolysis of APP. Proc Natl Acad Sci U S A 112:8445–8450.

Cotman SL, Vrbanac V, Lebel LA, Lee RL, Johnson KA, Donahue LR, Teed AM, Antonellis K, Bronson RT, Lerner TJ, MacDonald ME (2002) Cln3 (Deltaex7/8) knock-in mice with the common JNCL mutation exhibit progressive neurologic disease that begins before birth. Hum Mol Genet 11:2709–2721.

Dannhausen K, Mohle C, Langmann T (2018) Immunomodulation with minocycline rescues retinal degeneration in juvenile neuronal ceroid lipofuscinosis mice highly susceptible to light damage. Dis Model Mech 11: dmm033597.

Dasgupta S, Roy A, Jana M, Hartley DM, Pahan K (2007) Gemfibrozil ameliorates relapsing-remitting experimental autoimmune encephalomyelitis independent of peroxisome proliferator-activated receptor-alpha. Mol Pharmacol 72:934–946.

Dutta D, Jana M, Majumder M, Mondal S, Roy A, Pahan K (2021) Selective targeting of the TLR2/MyD88/NF-κB pathway reduces α-synuclein spreading *in vitro* and *in vivo*. Nat Commun 12:5382.

Ghosh A, Pahan K (2012) Gemfibrozil, a lipid-lowering drug, induces suppressor of cytokine signaling 3 in glial cells: implications for neurodegenerative disorders. J Biol Chem 287:27189–27203.

Ghosh A, Pahan K (2016) PPARα in lysosomal biogenesis: a perspective. Pharmacol Res 103:144–148.

Ghosh A, Corbett GT, Gonzalez FJ, Pahan K (2012) Gemfibrozil and fenofibrate, Food and Drug Administration-approved lipid-lowering drugs, up-regulate tripeptidyl-peptidase 1 in brain cells via peroxisome proliferator-activated receptor α: implications for late infantile Batten disease therapy. J Biol Chem 287:38922–38935.

Ghosh A, Jana M, Modi K, Gonzalez FJ, Sims KB, Berry-Kravis E, Pahan K (2015) Activation of peroxisome proliferator-activated receptor α induces lysosomal biogenesis in brain cells: implications for lysosomal storage disorders. J Biol Chem 290:10309–10324.

Ghosh A, Rangasamy SB, Modi KK, Pahan K (2017) Gemfibrozil, food and drug administration-approved lipid-lowering drug, increases longevity in mouse model of late infantile neuronal ceroid lipofuscinosis. J Neurochem 141:423–435.

Gottschalk CG, Jana M, Roy A, Patel DR, Pahan K (2021) Gemfibrozil protects dopaminergic neurons in a mouse model of Parkinson's disease via PPARα-dependent astrocytic GDNF pathway. J Neurosci 41:2287–2300.

Greene ND, Bernard DL, Taschner PE, Lake BD, de Vos N, Breuning MH, Gardiner RM, Mole SE, Nussbaum RL, Mitchison HM (1999) A murine model for juvenile NCL: gene targeting of mouse Cln3. Mol Genet Metab 66:309–313.

Groh J, Berve K, Martini R (2017) Fingolimod and teriflunomide attenuate neurodegeneration in mouse models of neuronal ceroid lipofuscinosis. Mol Ther 25:1889–1899.

Haltia M, Herva R, Suopanki J, Baumann M, Tyynelä J (2001) Hippocampal lesions in the neuronal ceroid lipofuscinoses. Eur J Paediatr Neurol 5 Suppl A:209–211.

Jana M, Pahan K (2012) Gemfibrozil, a lipid lowering drug, inhibits the activation of primary human microglia via peroxisome proliferator-activated receptor β. Neurochem Res 37:1718–1729.

Jana M, Jana A, Liu X, Ghosh S, Pahan K (2007) Involvement of phosphatidylinositol 3-kinase-mediated up-regulation of I kappa B alpha in anti-inflammatory effect of gemfibrozil in microglia. J Immunol 179:4142–4152.

Jana M, Palencia CA, Pahan K (2008) Fibrillar amyloid-beta peptides activate microglia via TLR2: implications for Alzheimer's disease. J Immunol 181:7254–7262.

Jana M, Mondal S, Gonzalez FJ, Pahan K (2012) Gemfibrozil, a lipid-lowering drug, increases myelin genes in human oligodendrocytes via peroxisome proliferator-activated receptor-β. J Biol Chem 287:34134–34148.

Johnson TB, Cain JT, White KA, Ramirez-Montealegre D, Pearce DA, Weimer JM (2019) Therapeutic landscape for Batten disease: current treatments and future prospects. Nat Rev Neurol 15:161–178.

Katz ML, Gao CL, Prabhakaram M, Shibuya H, Liu PC, Johnson GS (1997) Immunochemical localization of the Batten disease (CLN3) protein in retina. Invest Ophthalmol Vis Sci 38:2375–2386.

Kim K, Kleinman HK, Lee HJ, Pahan K (2017) Safety and potential efficacy of gemfibrozil as a supportive treatment for children with late infantile neuronal ceroid lipofuscinosis and other lipid storage disorders. Orphanet J Rare Dis 12:113.

Kovács AD, Pearce DA (2008) Attenuation of AMPA receptor activity improves motor skills in a mouse model of juvenile Batten disease. Exp Neurol 209:288–291.

Kyttälä A, Lahtinen U, Braulke T, Hofmann SL (2006) Functional biology of the neuronal ceroid lipofuscinoses (NCL) proteins. Biochim Biophys Acta 1762:920–933.

Lange J, Haslett LJ, Lloyd-Evans E, Pocock JM, Sands MS, Williams BP, Cooper JD (2018) Compromised astrocyte function and survival negatively impact neurons in infantile neuronal ceroid lipofuscinosis. Acta Neuropathol Commun 6:74.

Lovett-Racke AE, Hussain RZ, Northrop S, Choy J, Rocchini A, Matthes L, Chavis JA, Diab A, Drew PD, Racke MK (2004) Peroxisome proliferator-activated receptor alpha agonists as therapy for autoimmune disease. J Immunol 172:5790–5798.

Malik A, Kanneganti TD (2018) Function and regulation of IL-α in inflammatory diseases and cancer. Immunol Rev 281:124–137.

Martini-Stoica H, Xu Y, Ballabio A, Zheng H (2016) The autophagy-lysosomal pathway in neurodegeneration: A TFEB Perspective. Trends Neurosci 39:221–234.

Mirza M, Vainshtein A, DiRonza A, Chandrachud U, Haslett LJ, Palmieri M, Storch S, Groh J, Dobzinski N, Napolitano G, Schmidtke C, Kerkovich DM (2019) The CLN3 gene and protein: what we know. Mol Genet Genomic Med 7:e859.

Mitchison HM, Bernard DJ, Greene ND, Cooper JD, Junaid MA, Pullarkat RK, de Vos N, Breuning MH, Owens JW, Mobley WC, Gardiner RM, Lake BD, Taschner PE, Nussbaum RL (1999) Targeted disruption of the Cln3 gene provides a mouse model for Batten disease. The Batten Mouse Model Consortium [corrected]. Neurobiol Dis 6:321–334.

Mole SE, Cotman SL (2015) Genetics of the neuronal ceroid lipofuscinoses (Batten disease). Biochim Biophys Acta 1852:2237–2241.

Napolitano G, Ballabio A (2016) TFEB at a glance. J Cell Sci 129:2475–2481.

Pahan K, Sheikh FG, Namboodiri AM, Singh I (1998) N-acetyl cysteine inhibits induction of no production by endotoxin or cytokine stimulated rat peritoneal macrophages, C6 glial cells and astrocytes. Free Radic Biol Med 24:39–48.

Pahan K, Jana M, Liu X, Taylor BS, Wood C, Fischer SM (2002) Gemfibrozil, a lipid-lowering drug, inhibits the induction of nitric-oxide synthase in human astrocytes. J Biol Chem 277:45984–45991.

Paidi RK, Jana M, Mishra RK, Dutta D, Raha S, Pahan K (2021a) ACE-2-interacting domain of SARS-CoV-2 (AIDS) peptide suppresses inflammation to reduce fever and protect lungs and heart in mice: implications for COVID-19 therapy. J Neuroimmune Pharmacol 16:59–70.

Paidi RK, Jana M, Mishra RK, Dutta D, Pahan K (2021b) Selective inhibition of the interaction between SARS-CoV-2 Spike S1 and ACE2 by SPIDAR peptide induces anti-inflammatory therapeutic responses. J Immunol 207:2521–2533.

Palmer DN (2015) The relevance of the storage of subunit c of ATP synthase in different forms and models of Batten disease (NCLs). Biochim Biophys Acta 1852:2287–2291.

Parviainen L, Dihanich S, Anderson GW, Wong AM, Brooks HR, Abeti R, Rezaie P, Lalli G, Pope S, Heales SJ, Mitchison HM, Williams BP, Cooper JD (2017) Glial cells are functionally impaired in juvenile neuronal ceroid lipofuscinosis and detrimental to neurons. Acta Neuropathol Commun 5:74.

Patel D, Roy A, Kundu M, Jana M, Luan CH, Gonzalez FJ, Pahan K (2018) Aspirin binds to PPARα to stimulate hippocampal plasticity and protect memory. Proc Natl Acad Sci U S A 115:E7408–E7417.

Patel D, Jana A, Roy A, Pahan K (2019) Cinnamon and its metabolite protect the nigrostriatum in a mouse model of Parkinson's disease via astrocytic GDNF. J Neuroimmune Pharmacol 14:503–518.

Petcherski A, Chandrachud U, Butz ES, Klein MC, Zhao WN, Reis SA, Haggarty SJ, Ruonala MO, Cotman SL (2019) An autophagy modifier screen identifies small molecules capable of reducing autophagosome accumulation in a model of CLN3-mediated neurodegeneration. Cells 8:1531.

Pohl S, Mitchison HM, Kohlschutter A, van Diggelen O, Braulke T, Storch S (2007) Increased expression of lysosomal acid phosphatase in CLN3-defective cells and mouse brain tissue. J Neurochem 103:2177–2188.

Pontikis CC, Cotman SL, MacDonald ME, Cooper JD (2005) Thalamocortical neuron loss and localized astrocytosis in the Cln3Deltaex7/8 knock-in mouse model of Batten disease. Neurobiol Dis 20:823–836.

Raha S, Dutta D, Roy A, Pahan K (2020) Reduction of Lewy body pathology by oral cinnamon. J Neuroimmune Pharmacol 16:592–608.

Raha S, Ghosh A, Dutta D, Patel DR, Pahan K (2021) Activation of PPARα enhances astroglial uptake and degradation of β-amyloid. Sci Signal 14: eabg4747.

Rangasamy SB, Jana M, Roy A, Corbett GT, Kundu M, Chandra S, Mondal S, Dasarathi S, Mufson EJ, Mishra RK, Luan CH, Bennett DA, Pahan K (2018) Selective disruption of TLR2-MyD88 interaction inhibits inflammation and attenuates Alzheimer's pathology. J Clin Invest 128:4297–4312.

Rosenberg JB, Chen A, Kaminsky SM, Crystal RG, Sondhi D (2019) Advances in the treatment of neuronal ceroid lipofuscinosis. Expert Opin Orphan Drugs 7:473–500.

Roy A, Pahan K (2009) Gemfibrozil, stretching arms beyond lipid lowering. Immunopharmacol Immunotoxicol 31:339–351.

Roy A, Fung YK, Liu X, Pahan K (2006) Up-regulation of microglial CD11b expression by nitric oxide. J Biol Chem 281:14971–14980.

Roy A, Liu X, Pahan K (2007) Myelin basic protein-primed T cells induce neurotrophins in glial cells via alphavbeta3 [corrected] integrin. J Biol Chem 282:32222–32232.

Saha RN, Pahan K (2006) Regulation of inducible nitric oxide synthase gene in glial cells. Antioxid Redox Signal 8:929–947.

Shematorova EK, Shpakovski GV (2020) Current insights in elucidation of possible molecular mechanisms of the juvenile form of Batten disease. Int J Mol Sci 21:8055.

Specchio N, Ferretti A, Trivisano M, Pietrafusa N, Pepi C, Calabrese C, Livadiotti S, Simonetti A, Rossi P, Curatolo P, Vigevano F (2021) Neuronal ceroid lipofuscinosis: potential for targeted therapy. Drugs 81:101–123.

Sun A (2018) Lysosomal storage disease overview. Ann Transl Med 6:476.

Tyynelä J, Cooper JD, Khan MN, Shemilts SJ, Haltia M (2004) Hippocampal pathology in the human neuronal ceroid-lipofuscinoses: distinct patterns of storage deposition, neurodegeneration and glial activation. Brain Pathol 14:349–357.

Varghese NC, Macaden L, Premkumar B, Mathews P, Kumar S (2014) Delirium in older people in hospital: an education programme. Br J Nurs 23:704–709.

Wang H, Wang R, Carrera I, Xu S, Lakshmana MK (2016) TFEB overexpression in the P301S model of tauopathy mitigates increased PHF1 levels and lipofuscin puncta and rescues memory deficits. eNeuro 3: ENEURO.0042-16.2016.

Xiong J, Kielian T (2013) Microglia in juvenile neuronal ceroid lipofuscinosis are primed toward a pro-inflammatory phenotype. J Neurochem 127:245–258.